Diagnostics des plasmas produits par ablation laser à une interface liquide-solide.

D. Amans
Institut Lumière Matière

@ Fête des Lumières

Contents

time

Laser ablation in liquids attracts a broad interest

LIBS underwater

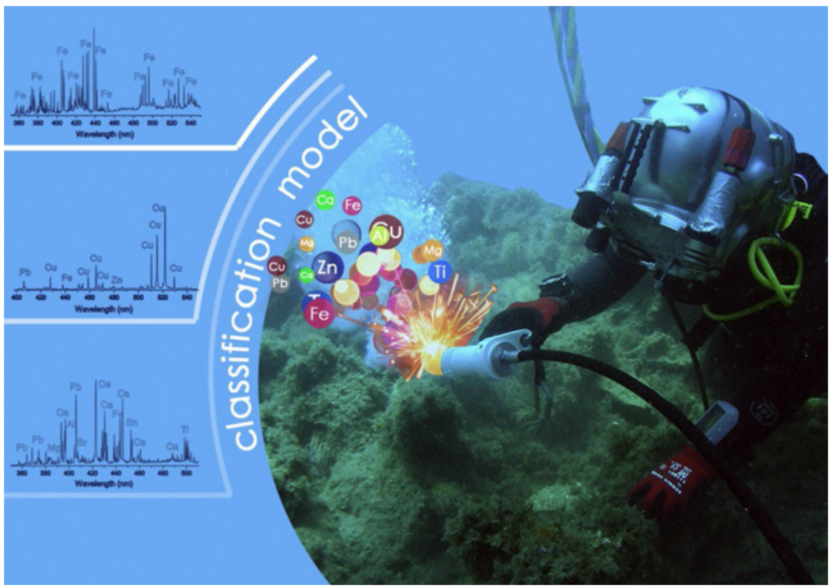

Interest: Geological exploration (oil industry)
Recognition of archeological materials…

M. López-Claros et al., J. Cultural Heritage 29, 75–81 (2018)

Laser ablation in liquids attracts a broad interest

Microfabrication

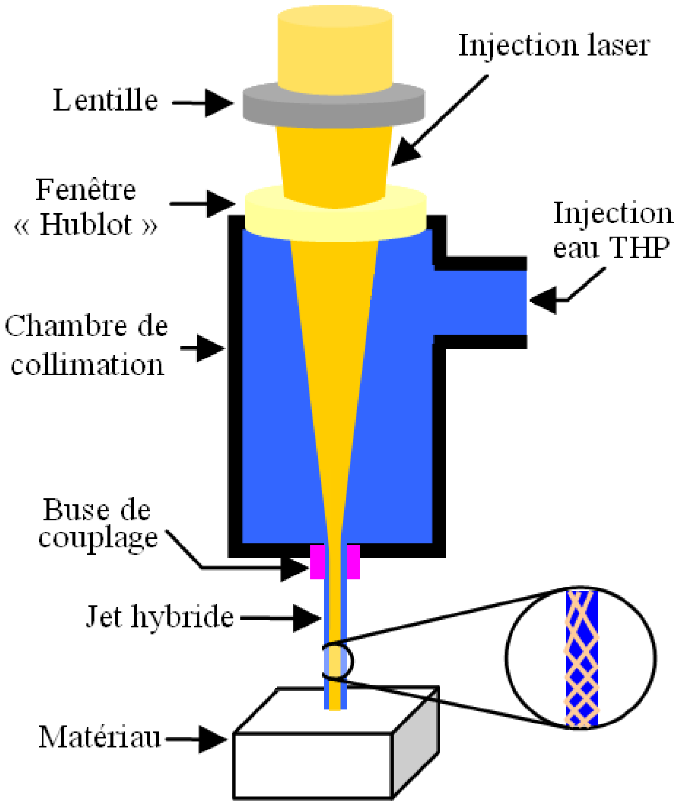

Thèse de Laurent Weiss, *Contribution au développement d'un procédé de découpe laser haute-énergie/ jet d'eau haute-pression couplés. Application à la découpe d'alliages métalliques*. Univ. Lorraine 5 juillet 2013

https://www.sugino.com/site/water-jet-and-laser-machine-e/

Laser ablation in liquids attracts a broad interest

Laser generation of colloids

Interest: one step process, particles with surface free of ligands, versatile…

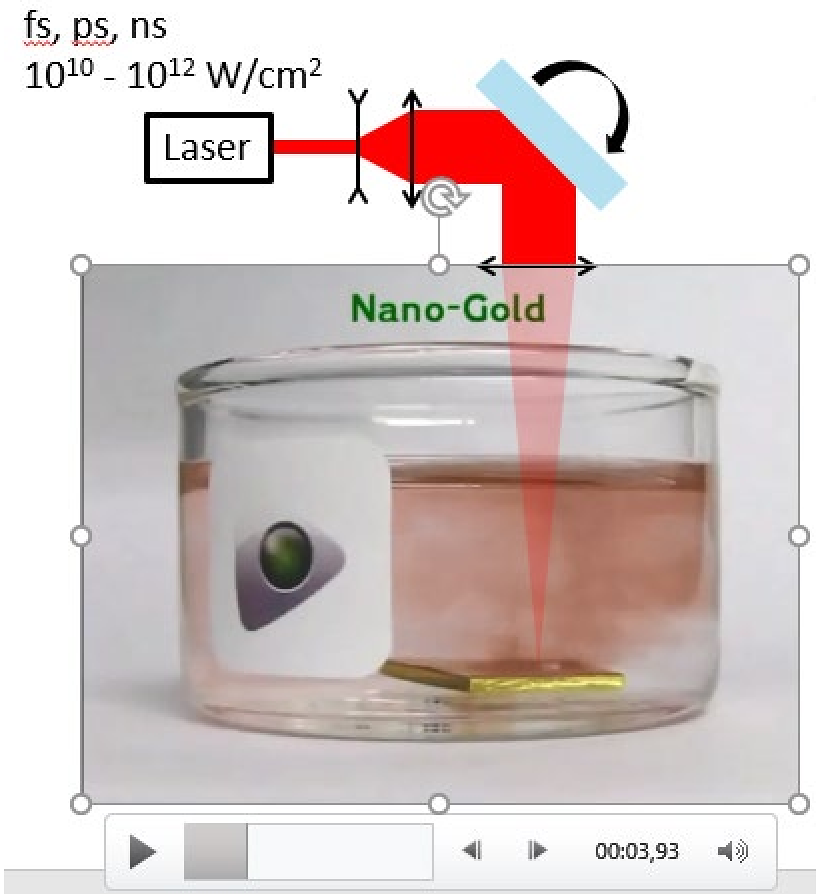

@ Particular GmbH

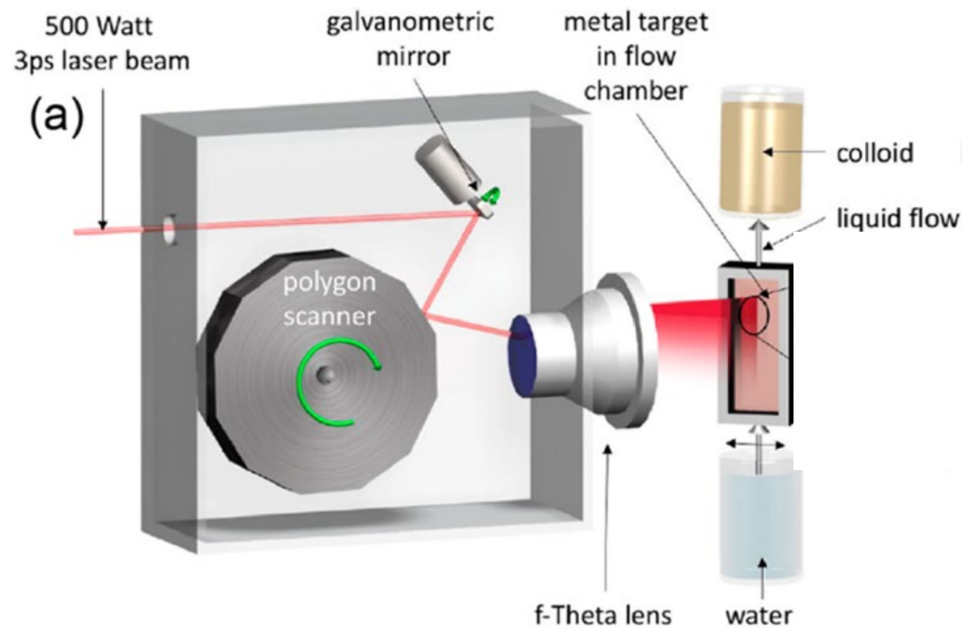

Productivity > 1g/hour (Pt, Au, Ag, Al, Cu, Ti)

R. Streubel *et al.*,, Opt. Lett. **41**, 1486–1489 (2016).
R Streubel *et al.*, *Nanotechnology* **27**, 205602 (2016).

Laser generation of colloids

Continuous flow setup

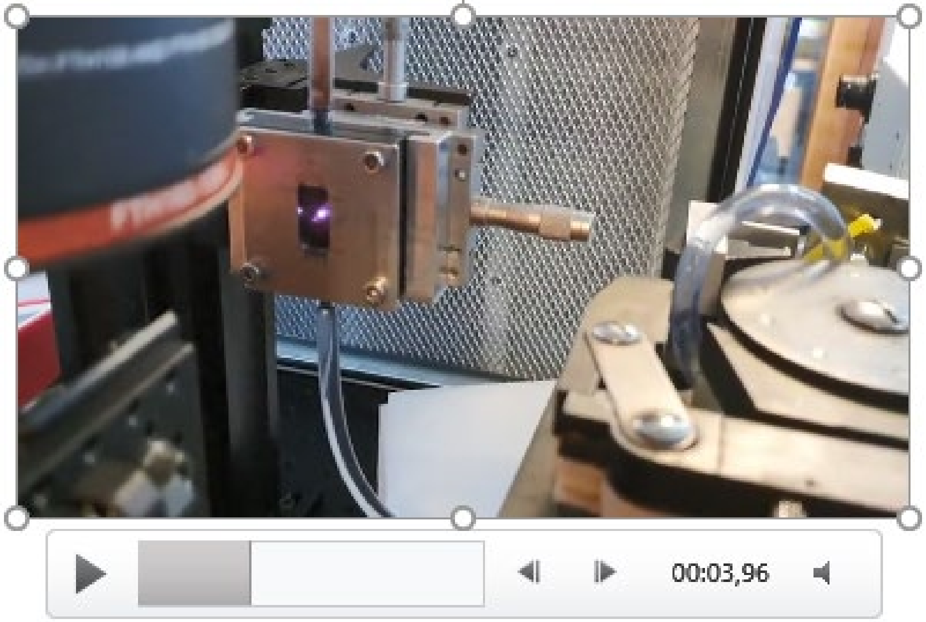

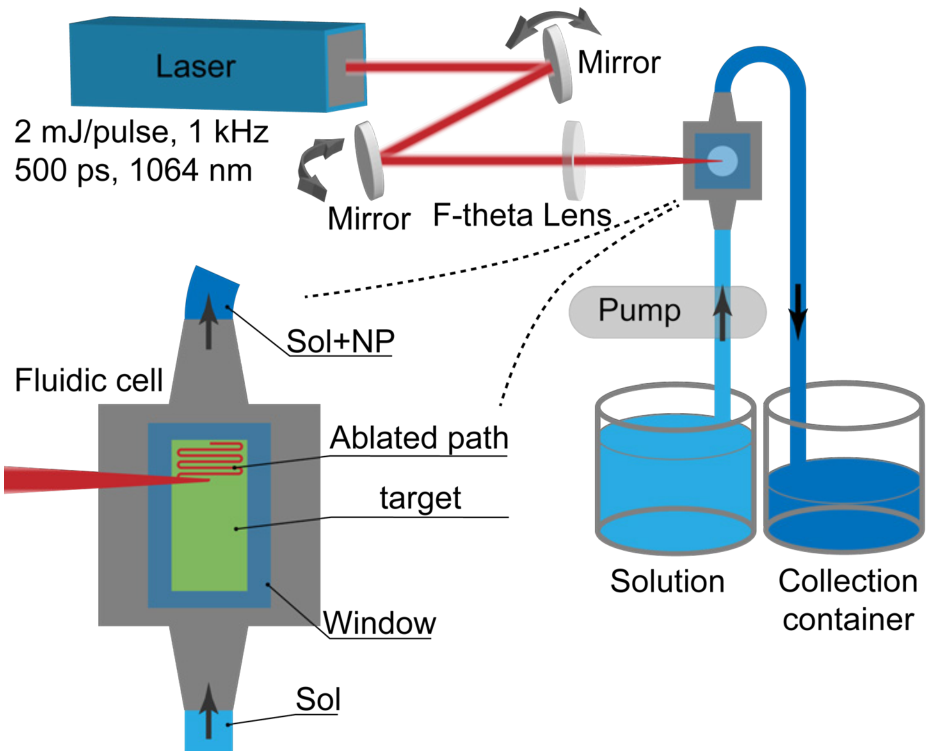

Productivity 15 – 40 mg/hour

Characteristic time scales in laser ablation

- **Overview**
- **Molecular dynamics**

Shadowgraph imaging using a fast camera (210 000 fps)

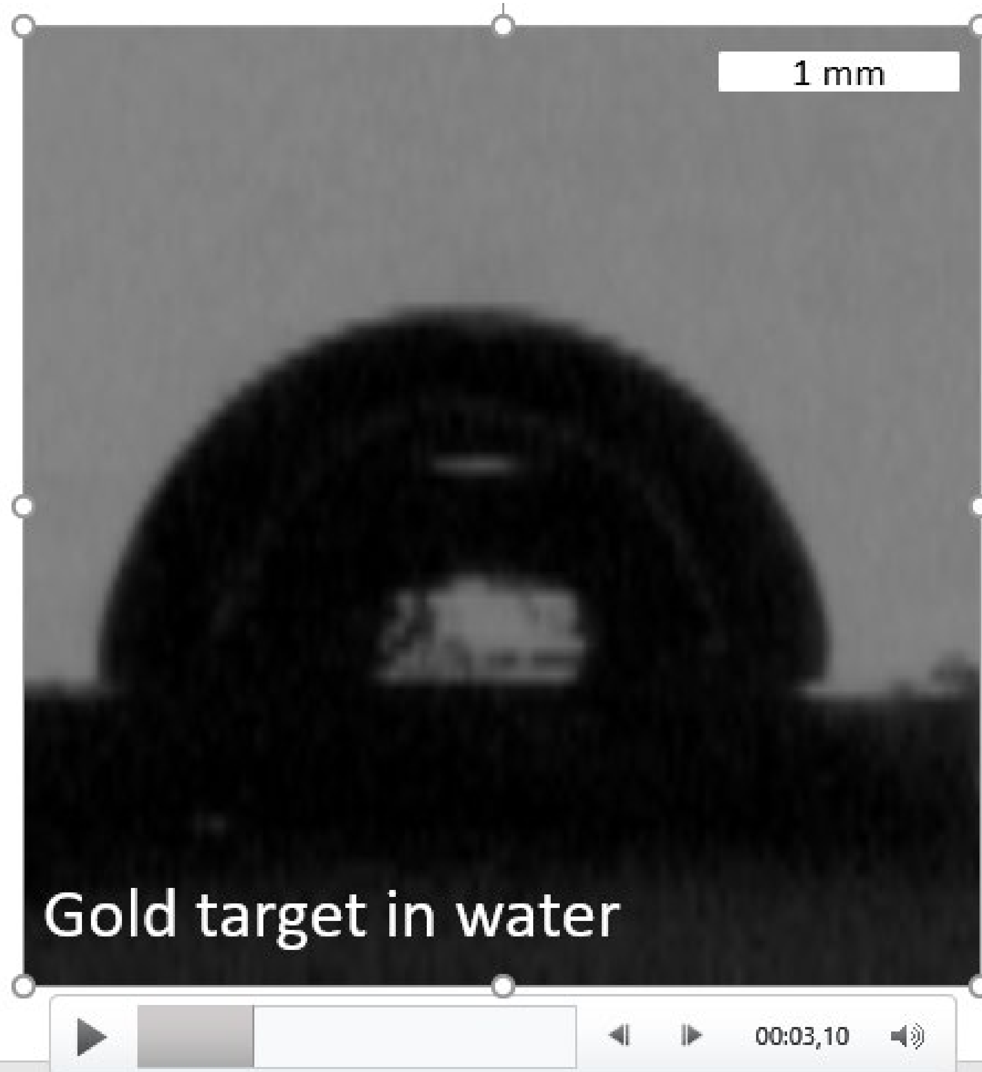

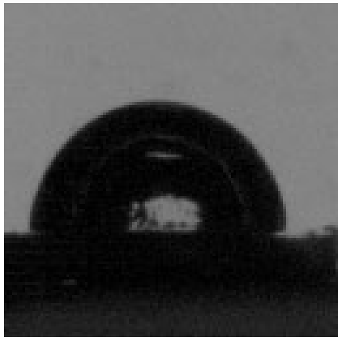

Characteristic time scales

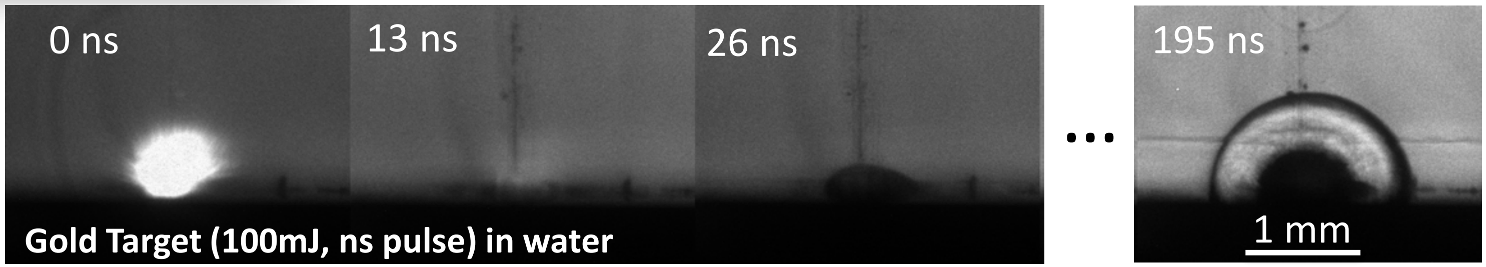

Shadowgraph imaging using a SIMX camera (16 iCCD, Gate 5ns).

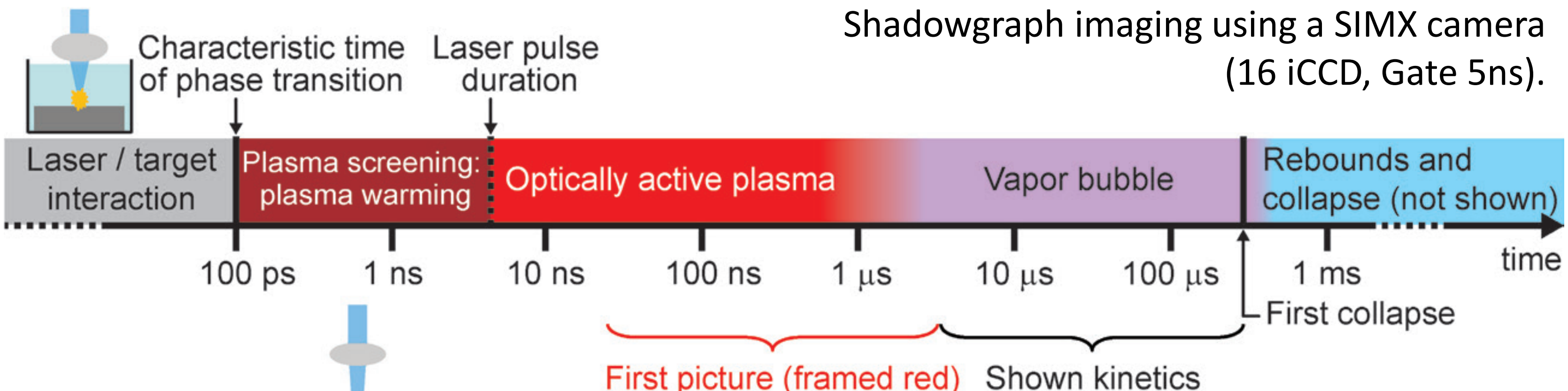

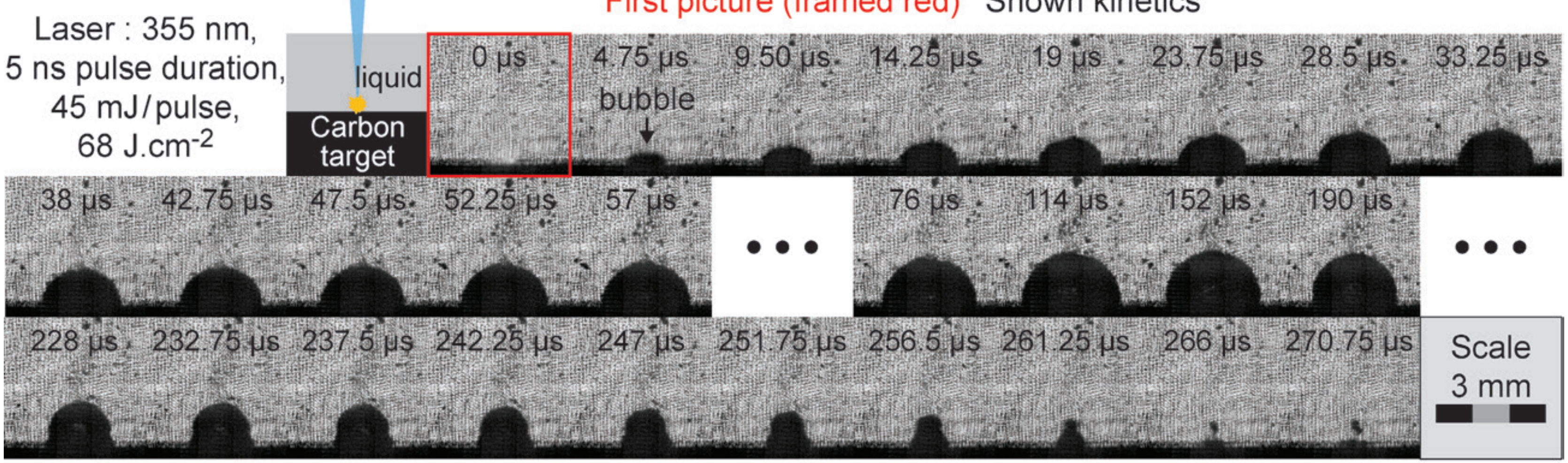

Shadograph imaging with fast camera

Amans *et al.*, J. Colloid. Interface Sci. **489**, 114-125 (2017).

Characteristic time scales

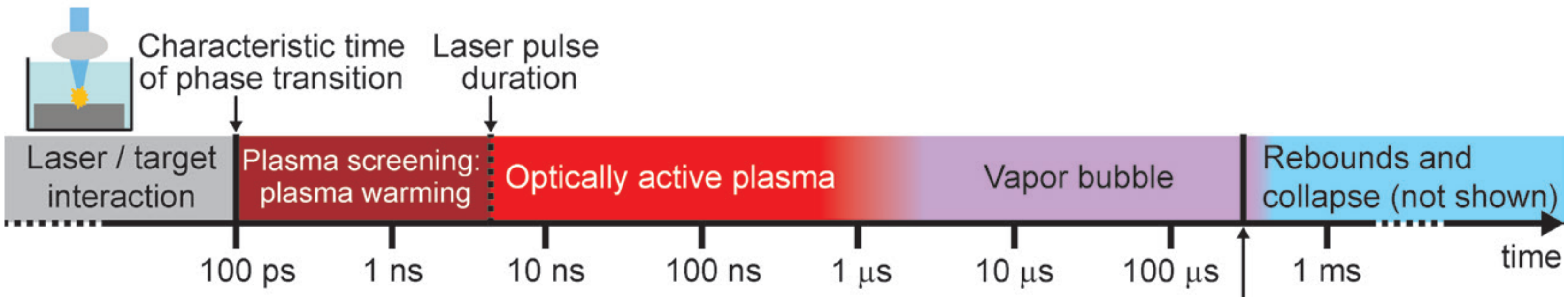

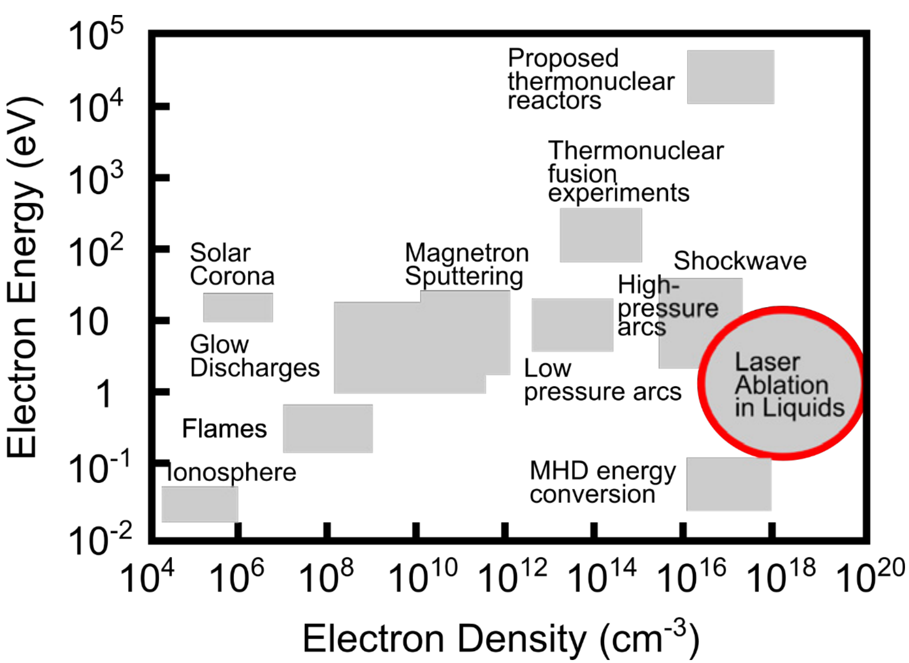

Original condition:

- **High pressure / Laser shock peening**
- **Fast cooling (a few µs vs. a few tens of µs in air)**
- **New category of plasma (T_e, N_e)**
- **Plasma-liquid interaction ?**
- **Original Cavitation (high Re, We and Ca)**

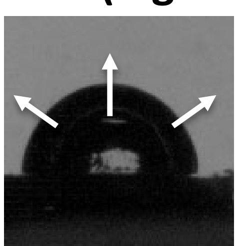

A. Kanitz et al., Plasma Sources Sci. Technol. 28, 103001 (2019).

In-situ characterization

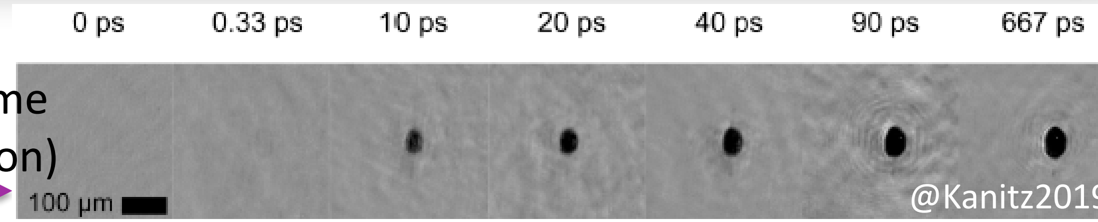

Pump-probe microscopy [24-25] (charac. time e-/phonon, heat diffusion, phase transition)

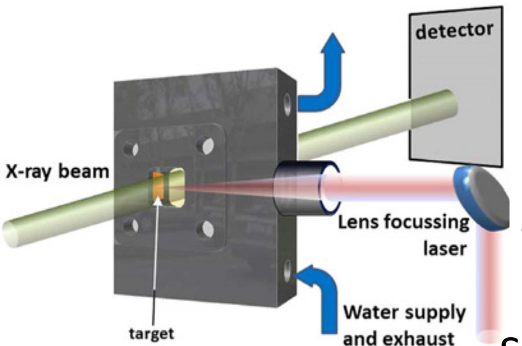

@Ibrahimkutty2015

Rayleigh-Mie scattering[12,13] (density, growth kinetics), Raman[19] (crystal structure)

small angle X-ray scattering [1,18] (particles diameter larger than few nm)

Shadowgraph[21,22] and Schlieren imaging[23] (shock waves)

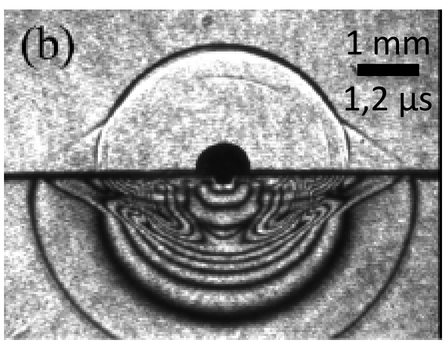

@Nguyen2013

acoustic signals[9-11] (shock waves release, cavitation lifetime)

Plasma Imagery [3-5,17] and shadowgraph fast imaging [2, 6-9,20] (P, V…)

Plasma spectroscopy[12,14-16] (species, T, electron density …)

Light induced fluorescence (species, T)

In-situ characterization

(1) S. Ibrahimkutty *et al.*, Appl. Phys. Lett. **101**, 103104 (2012) / S. Ibrahimkutty et al., Sci. Rep. **5**, 16313 (2015).
(2) T. Sakka *et al.*, Spectrochim. Acta, Part B **64**, 981 (2009).
(3) H. Oguchi *et al.*, J. Appl. Phys. **102**, 023306 (2007).
(4) K. Saito *et al.*, Appl. Surf. Sci. **197**, 56 (2002).
(5) B. Kumar *et al.*, J. Appl. Phys. **108**, 064906 (2010).
(6) K. Hirata *et al.*, Photon Proc. Microelec. Photonics IV, 2005, p. 311.
(7) T. Tsuji *et al.*, Jpn. J. Appl. Phys. **46**, 1533 (2007).
(8) K. Sasaki *et al.*, Pure Appl. Chem. **82**, 1317 (2010).
(9) T. Tsuji *et al.*, Appl. Surf. Sci. **254**, 5224 (2008).
(10) H. Jin *et al.*, Phys. Chem. Chem. Phys. **12**, 5199–5202 (2010).
(11) Zhu *et al.*, J. Appl. Phys. **89**, 2400 (2001)
(12) B. Kumar *et al.*, J. Appl. Phys. **110**, 074903 (2011).
(13) W. Soliman *et al.*, Appl. Phys. Express **3**, 035201 (2010).
(14) See bibliography of Tetsuo Sakka @ Kyoto University and Bhupesh Kumar @ Indian Institute of Technology Kanpur,
(15) J. Lam *et al.*, Phys.Chem.Chem.Phys. **16**, 963 (2014)
(16) A. Matsumoto *et al.*, J. Phys. Chem. C **119**, 26506 (2015).
(17) A. Tamura *et al.*, J. Appl. Phys. **117**, 173304 (2015).
(18) See bibliography of A. Pletch @ Karlsruhe Institute of Technology
(19) M. Takeuchi and K. Sasaki, Appl. Phys. A **122**, 312 (2016).
(20) J. Lam *et al.*, Appl. Phys. Lett. **108**, 074104 (2016)
(21) T.T.P. Nguyen et al., Appl. Phys. Lett. 102, 124103 (2013) / T.T.P. Nguyen et al., Optics and Laser Technology **100,** 21–26 (2018)
See bibliography of T. T. P. Nguyen @Nagaoka Univ. of Technology and then @Institute of Research and Development, Duy Tan Univ.
(22) Z. Zhang et al., AIP Advances 9, 125048 (2019)
(23) L. Martí-López et al., Appl. Opt. **48**, 3671 (2009)
(24) M. Domke et al., Appl. Phys A **109**, 409 (2012) / See bibliography of Heinz P. Huber @ Munich University of Applied Sciences
(25) A. Kanitz et al., Appl. Surf. Sci. **475,** 204 (2019).
[25bis] S. Rapp, M. Kaiser, M. Schmidt, H.P. Huber, Ultrafast pump-probe ellipsometry setup for the measurement of transient optical properties during laser ablation, Opt.Express 24 (16) (2016) 17572–17592, https://doi.org/10.1364/OE.24.017572.

Non-exhaustive list !
Ask me !

Characteristic time scales in laser ablation

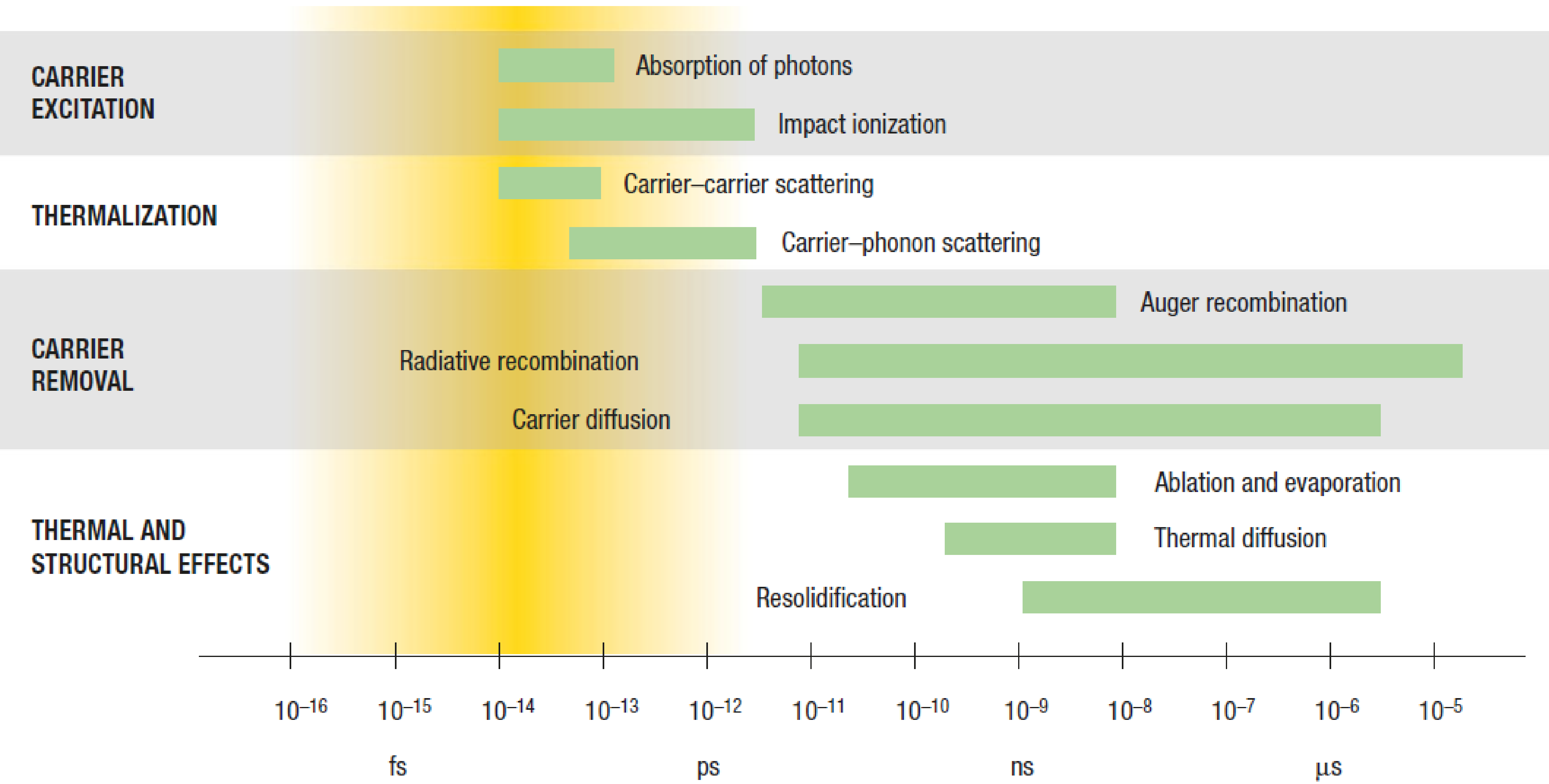

S. K. Sundaram et al., nature materials 1, 217 (2002)

Characteristic time scales in laser ablation

Ag target, 400ps, 600 mJ/cm^2, box size 50 nm x 50 nm
Molten Ag (blue) / Vapor-phase Ag atoms (red)

- ✓ **Early appearance of the nanoparticles (first few ns).**
- ✓ **Bimodal size distribution: Two mechanisms of nanoparticle generation in laser ablation in liquids.**

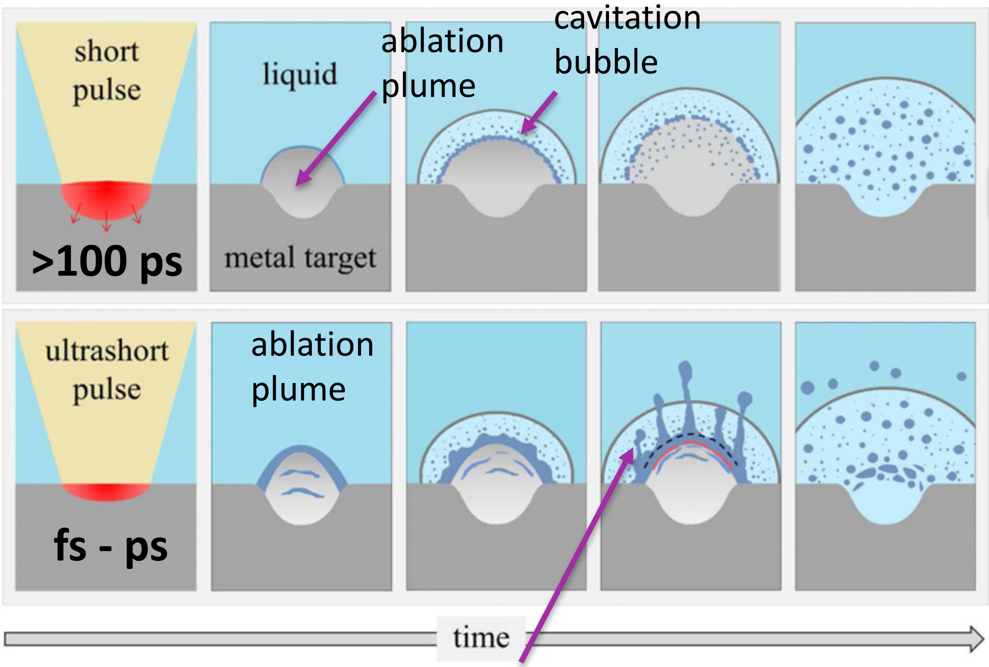

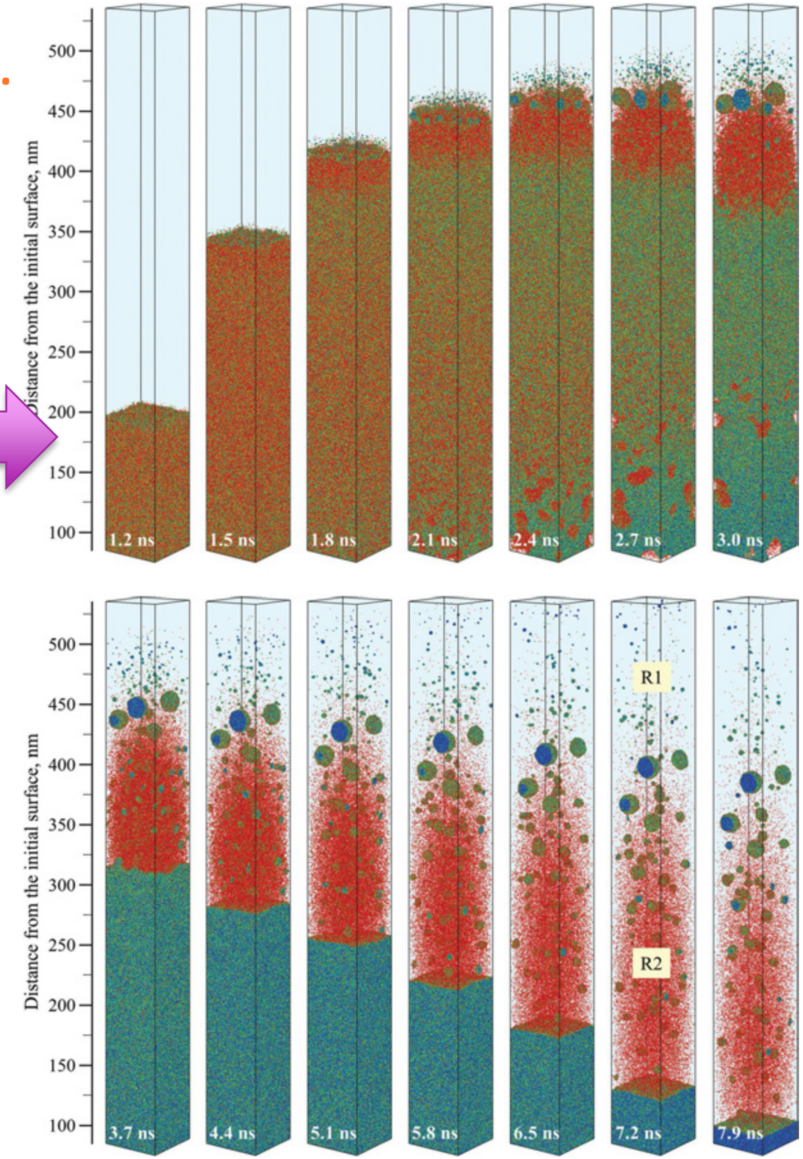

Jetting of the molten metal (Richtmyer–Meshkov instability) from the layer roughened by Rayleigh–Taylor instability

See bibliography of C.-Y. Shih & L. V. Zhigilei @ University of Virginia

Characteristic time scales in laser ablation

Basic question: Why do we observe multimodal size distribution even in $\underbrace{\text{flow chamber}}_{\text{No post-processes}}$?

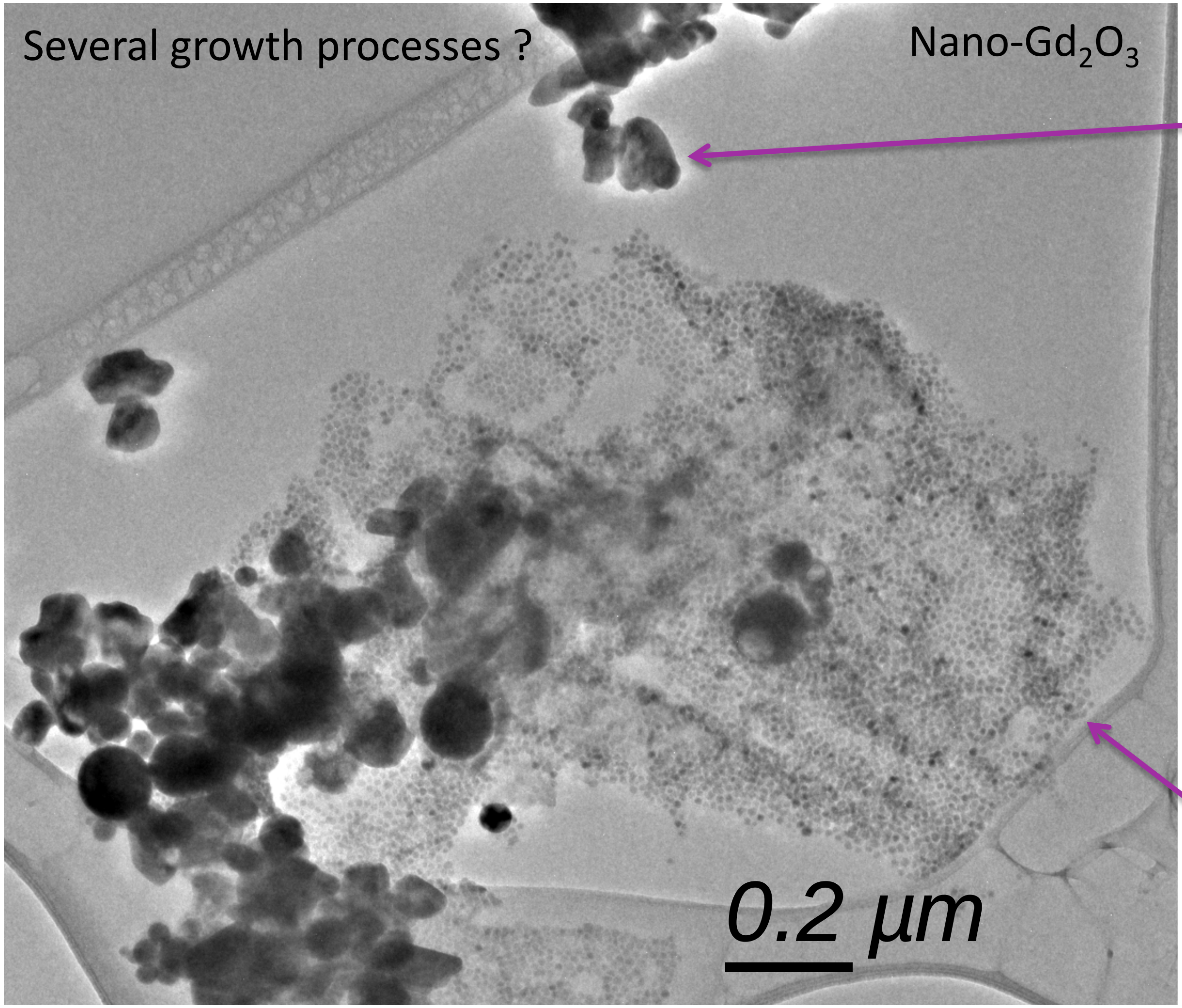

"Big" particles: Phase transition of the target (lift-off) ?

"Small" particles: Nucleation and growth from the plasma ?

Contents

Shock waves

- **Shock waves kinetics and pressure measurement**
- **Fabbro & Berthe’s model**
- **Surface waves and elastic modulus measurement**

Bibliography: Alfred Vogel (Univ. Lübeck) , Werner Lauterborn (Univ. Göttingen)

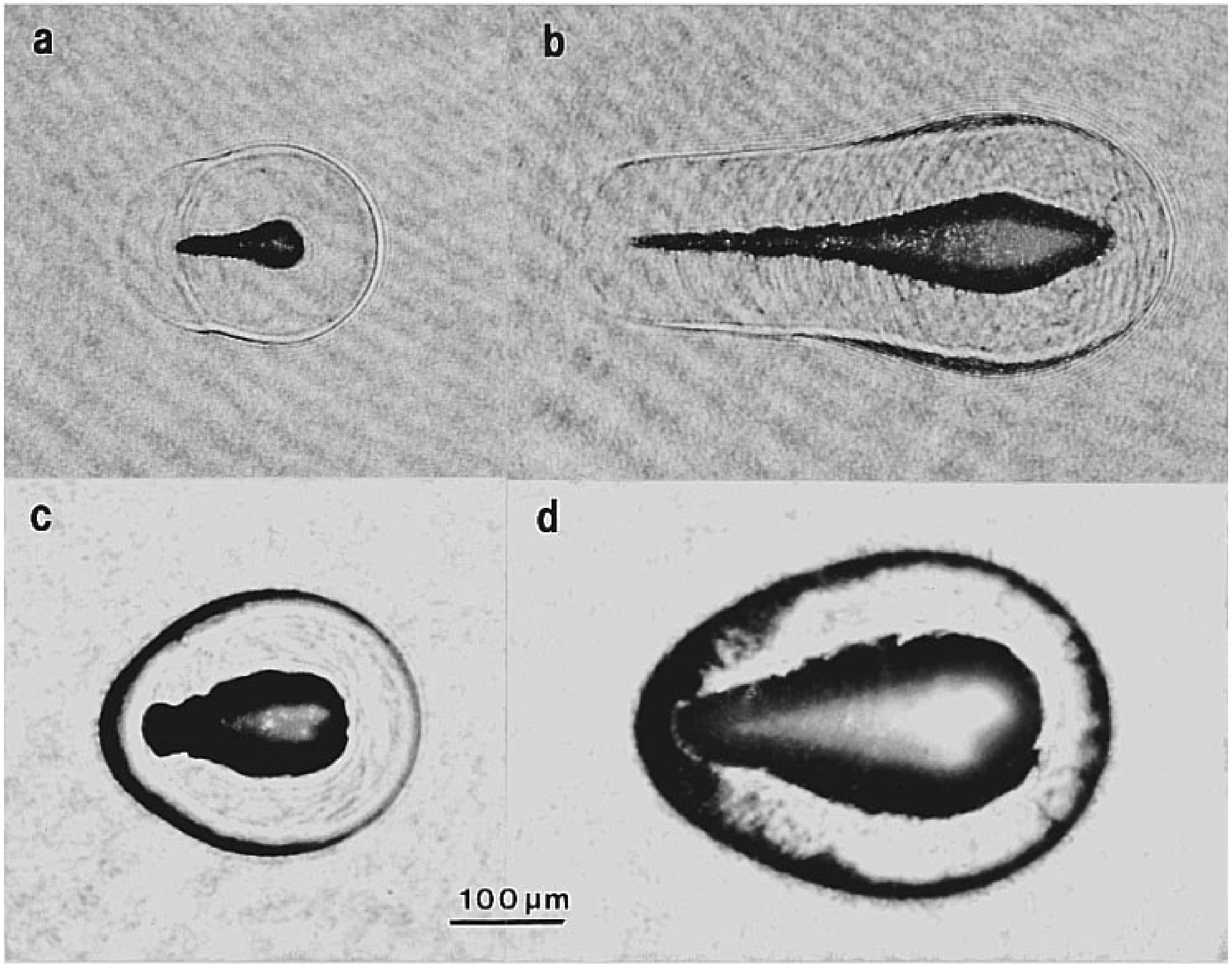

Plasma, shock wave, and cavitation bubble produced by Nd:YAG laser pulses of different duration and energy:

(a) 30 ps, 50 µJ;
(b) 30 ps, 1 mJ;
(c) 6 ns, 1 mJ;
(d) 6 ns, 10 mJ.

All pictures were taken **44 ns** after the optical breakdown.

A. Vogel, S. Busch, U. Parlitz, *Shock wave emission and cavitation bubble generation by picosecond and nanosecond optical breakdown in water*, J. Acoust. Soc. Am. 100, 148 (1996).

Shock waves

Laser pulse (5ns, > 10^{10} W/cm^2) → Phase transition → Large Pressure (GPa) → Shock-waves

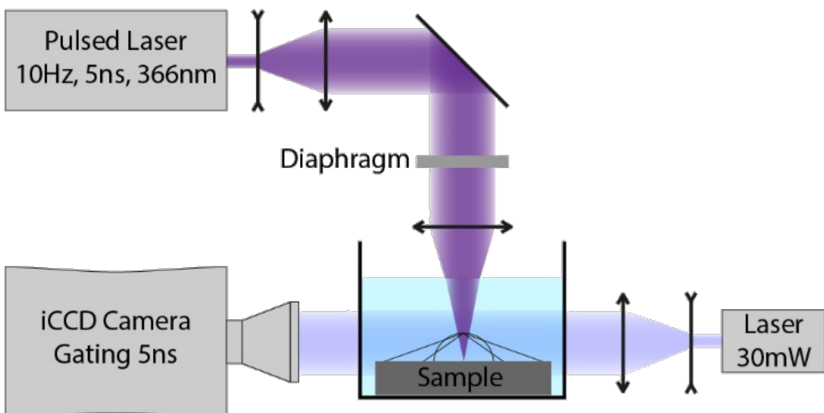

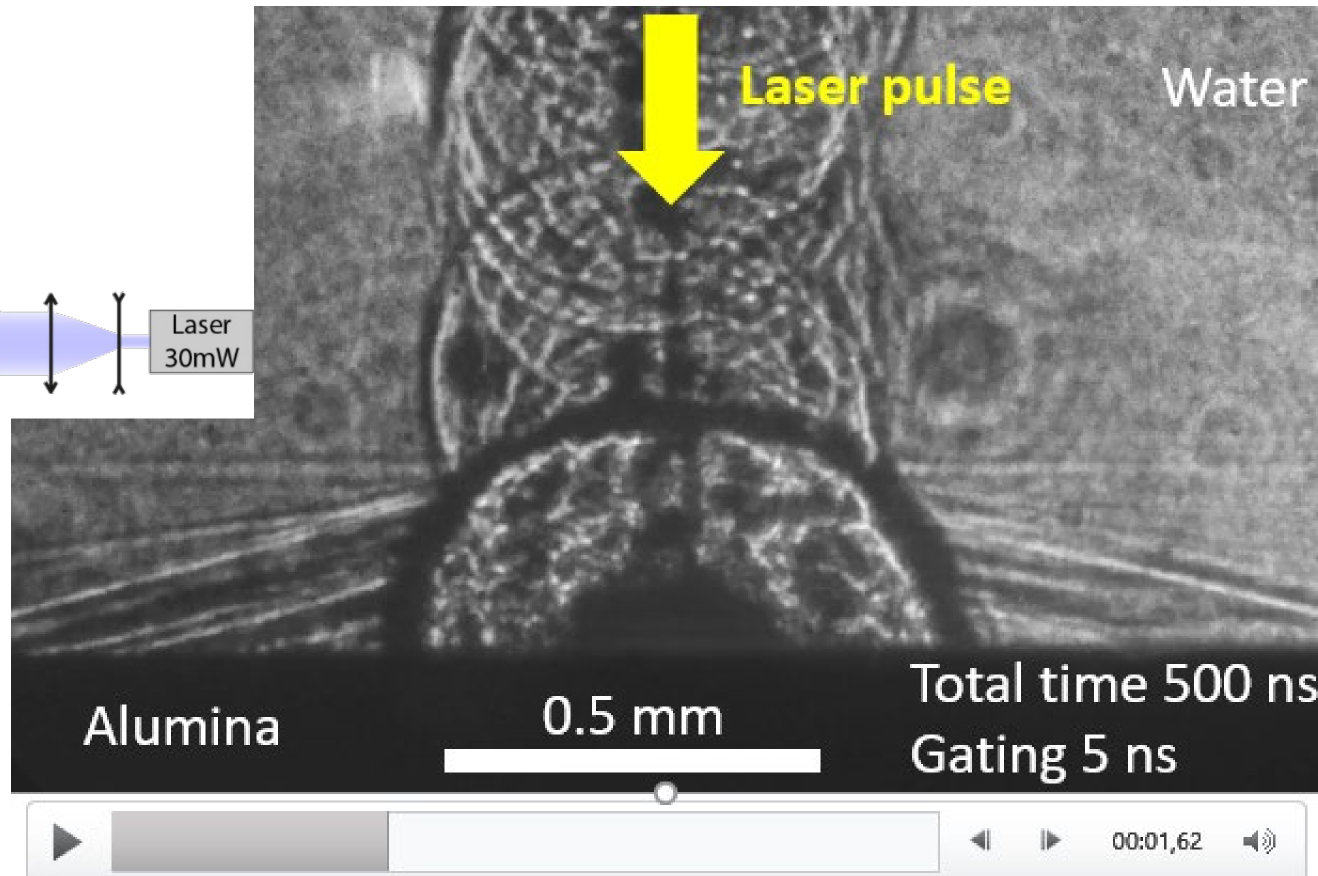

Shock front kinematics

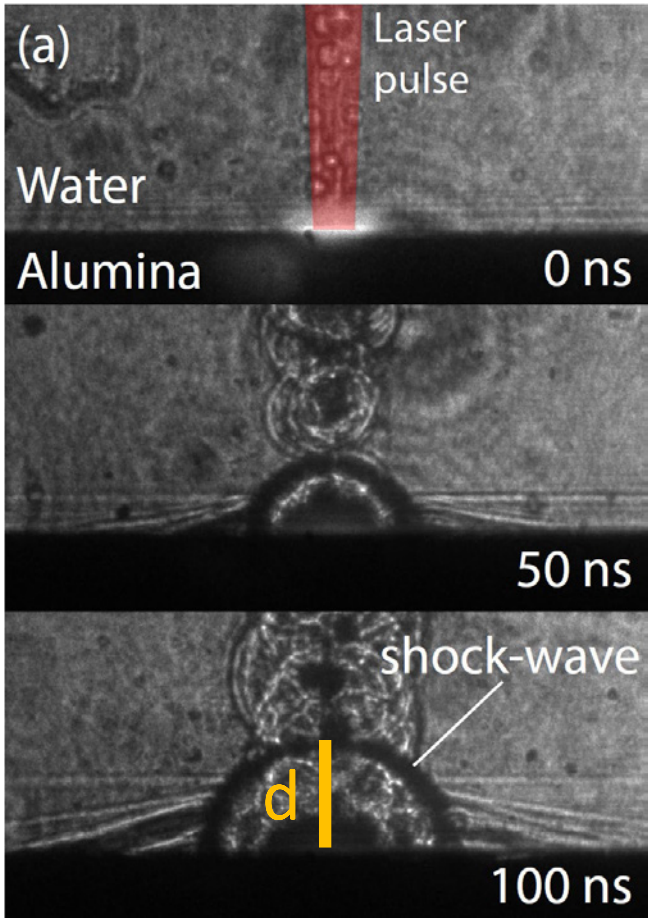

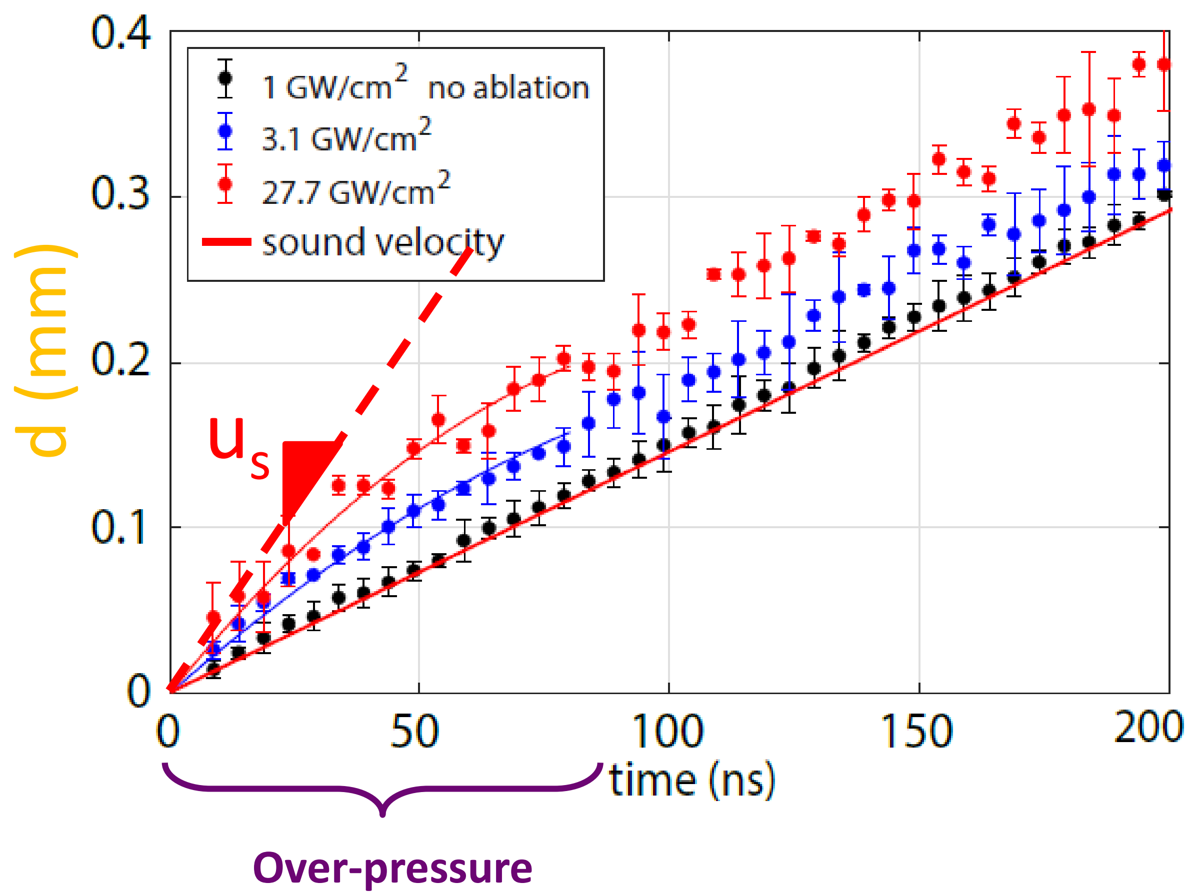

A. Chemin et al., Appl. Surf. Sci **574**, 151592 (2022)

Shock waves

Conservation of momentum at a shock front:

$p_s - p_\infty = u_s u_p \rho_0$

u_p : particles velocity

Hugoniot curve from Rice and Walsh:

$u_p = c_1\left(10^{\frac{u_s - c_0}{c_2}} - 1\right)$

$c_1 = 5190$ m/s ; $c_2 = 25\,306$ m/s

Valid up to 25 GPa

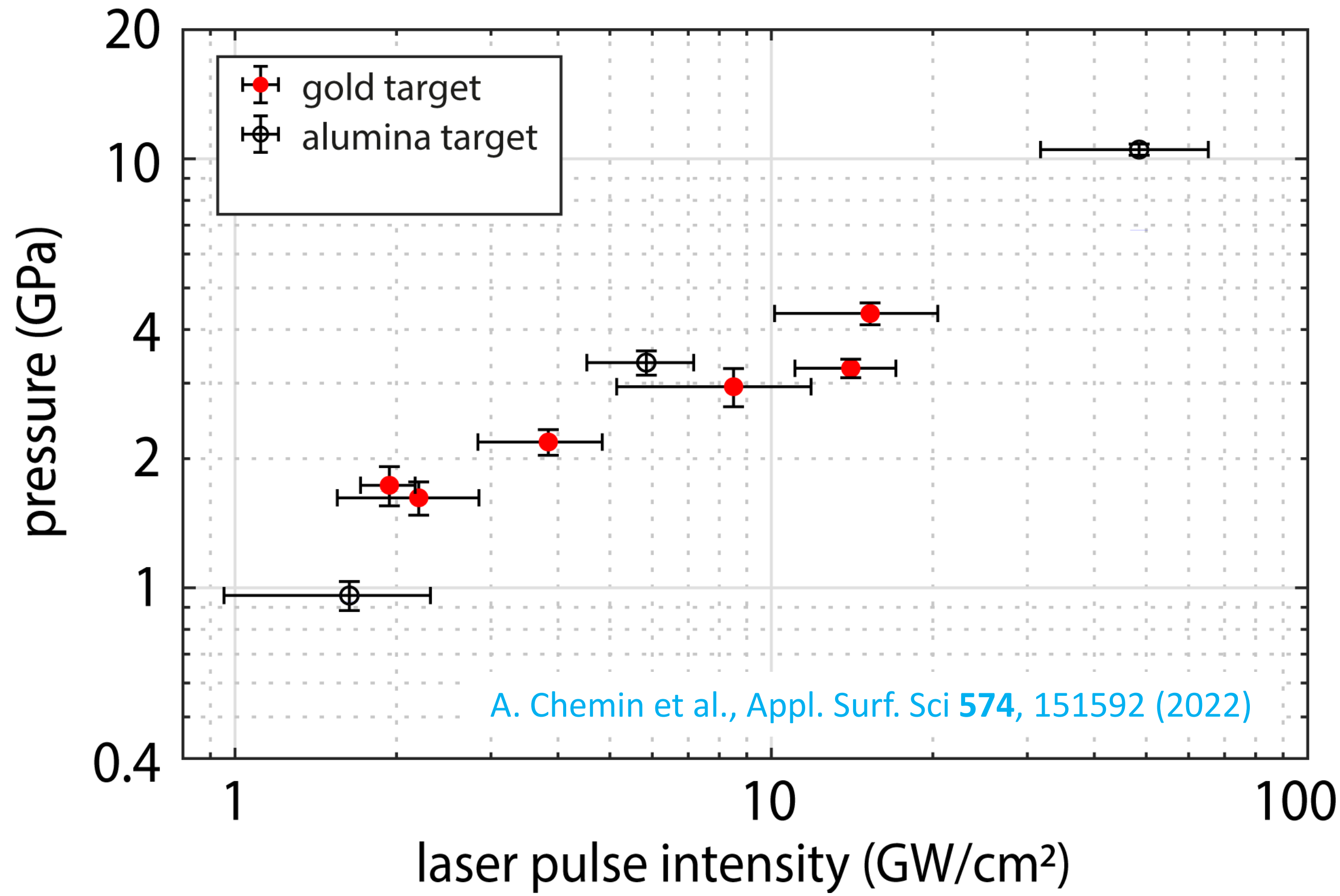

Relates the initial pressure to the pulse energy : $p_s(MPa) = 10\sqrt{\frac{a}{2a+3}ZI}$

R. Fabbro et al. J. Appl. Phys. **68**, 775 (1990)

Z the reduced acoustic impedance

I the laser intensity [W/cm²]

a fraction of pulse energy involved in the thermal energy

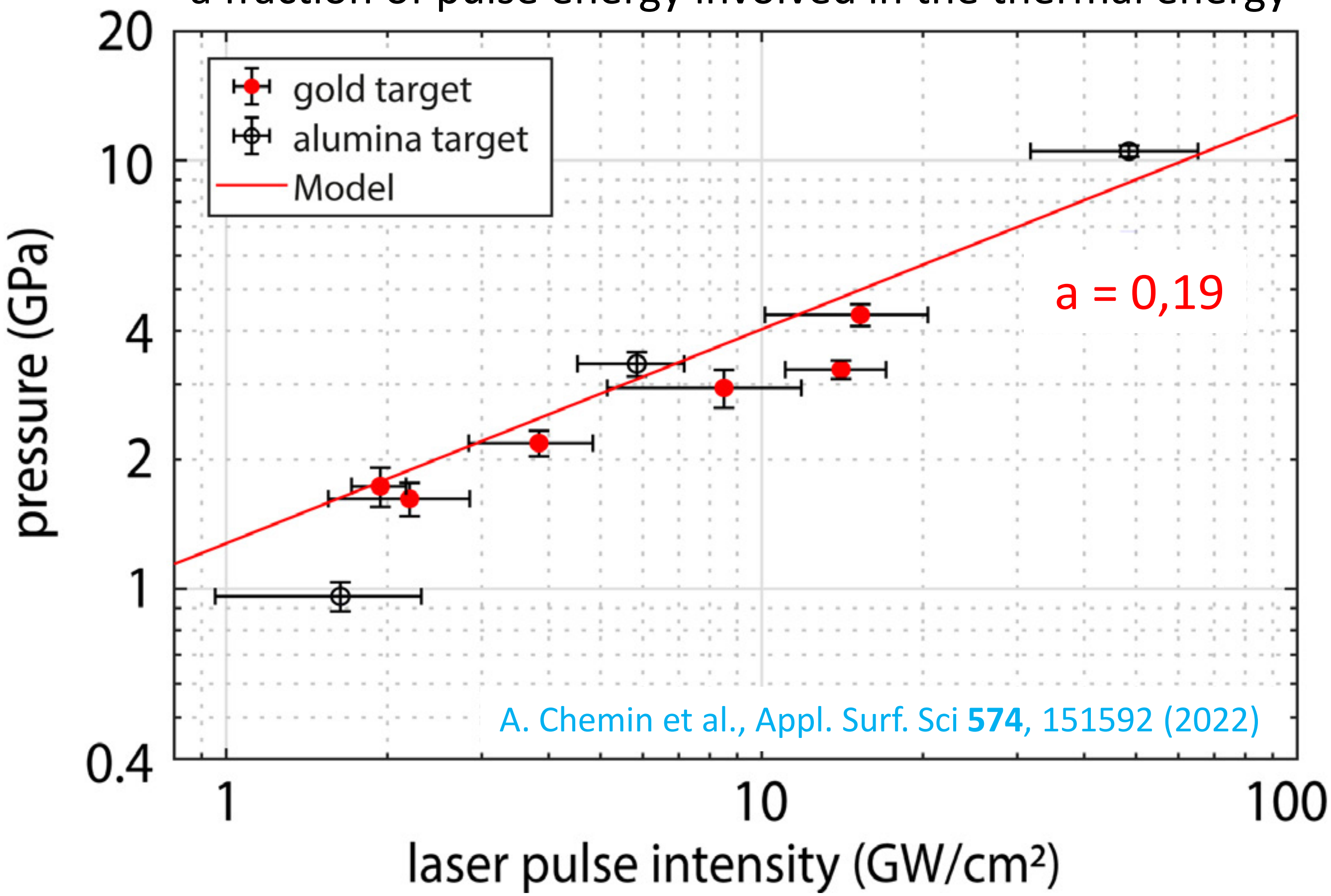

A. Chemin et al., Appl. Surf. Sci **574**, 151592 (2022)

Origin the observed shock waves ?

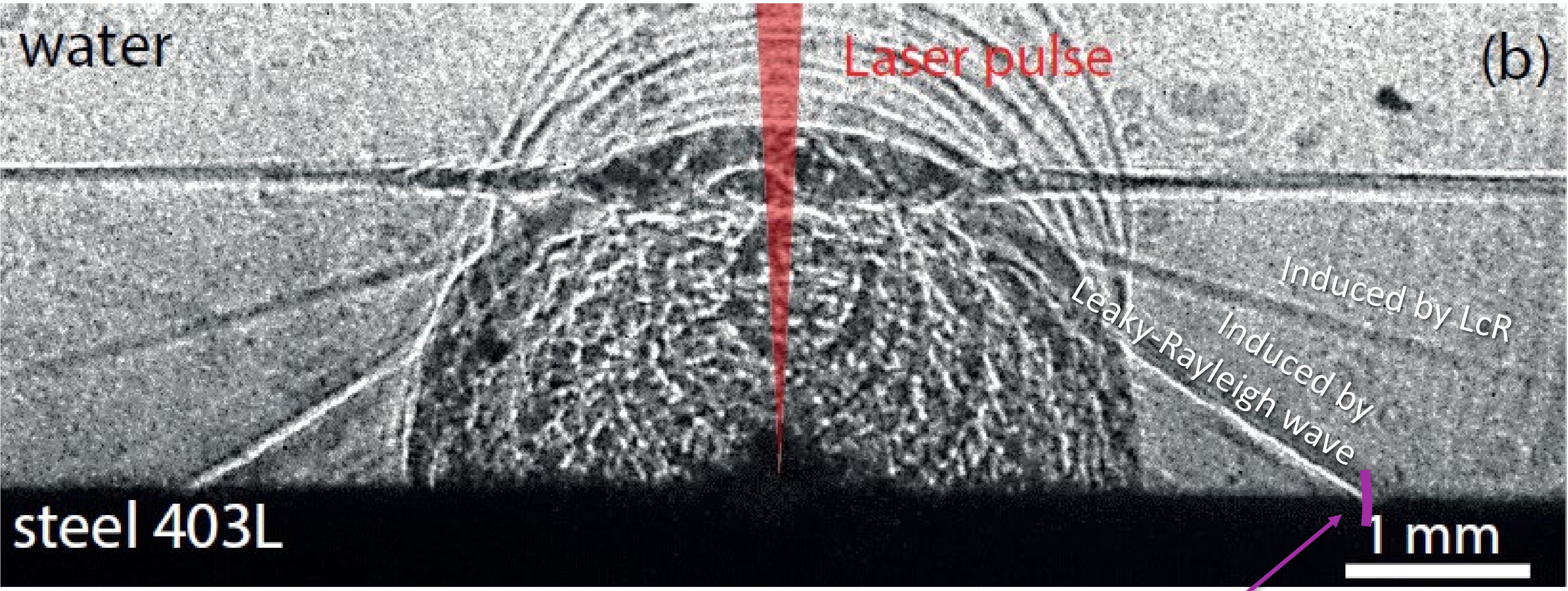

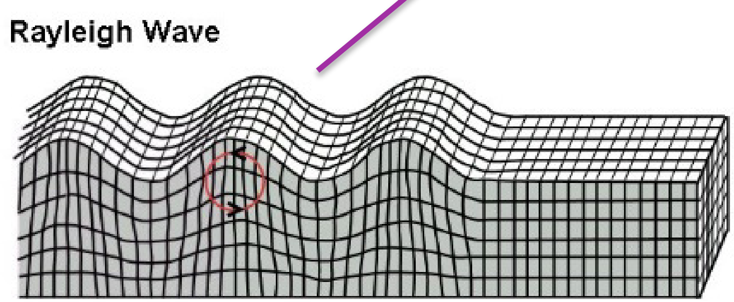

<u>“Mach” cone induced by:</u>

→ **Critically refracted longitudinal (LCR) wave**

→ **Surface waves** at the interface between the liquid and the target: the leaky-Rayleigh wave

Measurement of elastic modulus (E, ν)

Leaky Rayleigh wave

LcR

Measurement

$$\sin(\theta_R) = \frac{c_0}{c_R}$$

$$\sin(\theta_L) = \frac{c_0}{c_L}$$

c_0 sound velocity

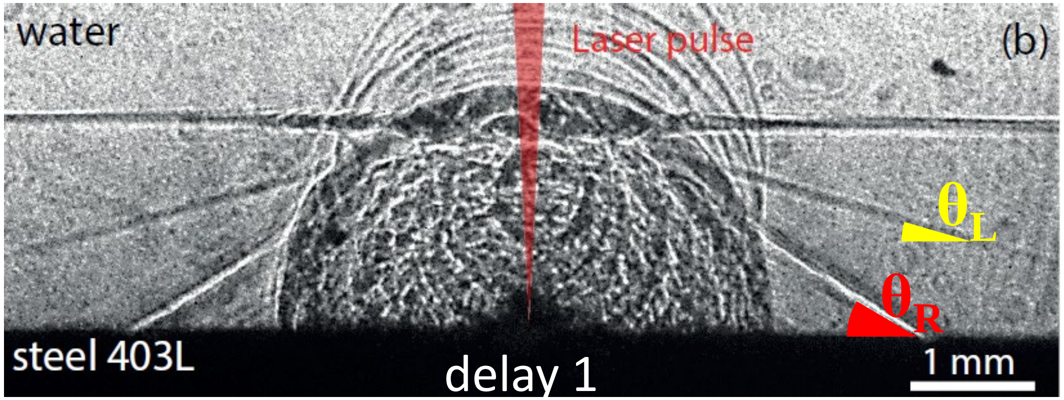

Rayleigh's approx.

In vacuum:

$$c_R = c_T\sqrt{\frac{28\nu + 22}{21\nu + 29}}$$

Wave velocities vs elastic modulus

For isotropic materials:

$$c_T = \sqrt{\frac{1}{2(1+\nu)}\frac{E}{\rho}} \qquad c_L = \sqrt{\frac{1-\nu}{(1+\nu)(1-2\nu)}\frac{E}{\rho}}$$

A. chemin, M. Fawaz, T. Vidril et D. Amans : « Procédé de mesure d'un module d'élasticité par génération laser d'ondes de surface à une interface matériau/liquide », demande de brevet français n° 2105079 déposée le 14 mai 2021.

Measurement of elastic modulus (E, ν)

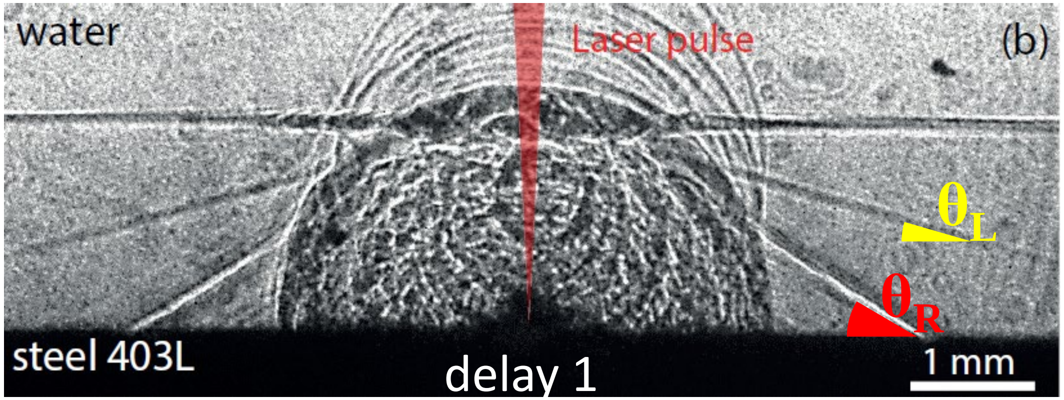

Measurement

$$\sin(\theta_R) = \frac{c_0}{c_R}$$

$$\sin(\theta_L) = \frac{c_0}{c_L}$$

Determination of ν

$$\left(\frac{\sin(\theta_L)}{\sin(\theta_R)}\right)^2 = \frac{1-2\nu}{2(1-\nu)} \times \frac{28\nu+22}{21\nu+29}$$

Determination of E/ρ

$$\frac{E}{\rho} = \frac{(1+\nu)(1-2\nu)}{1-\nu}\left(\frac{c_0}{\sin(\theta_L)}\right)^2$$

Depends only on the angles!

A. chemin, M. Fawaz, T. Vidril et D. Amans : « Procédé de mesure d'un module d'élasticité par génération laser d'ondes de surface à une interface matériau/liquide », demande de brevet français n° 2105079 déposée le 14 mai 2021.

Plasma/liquid interaction and bubble formation

Shock-bag @ ESRF (July 2023)

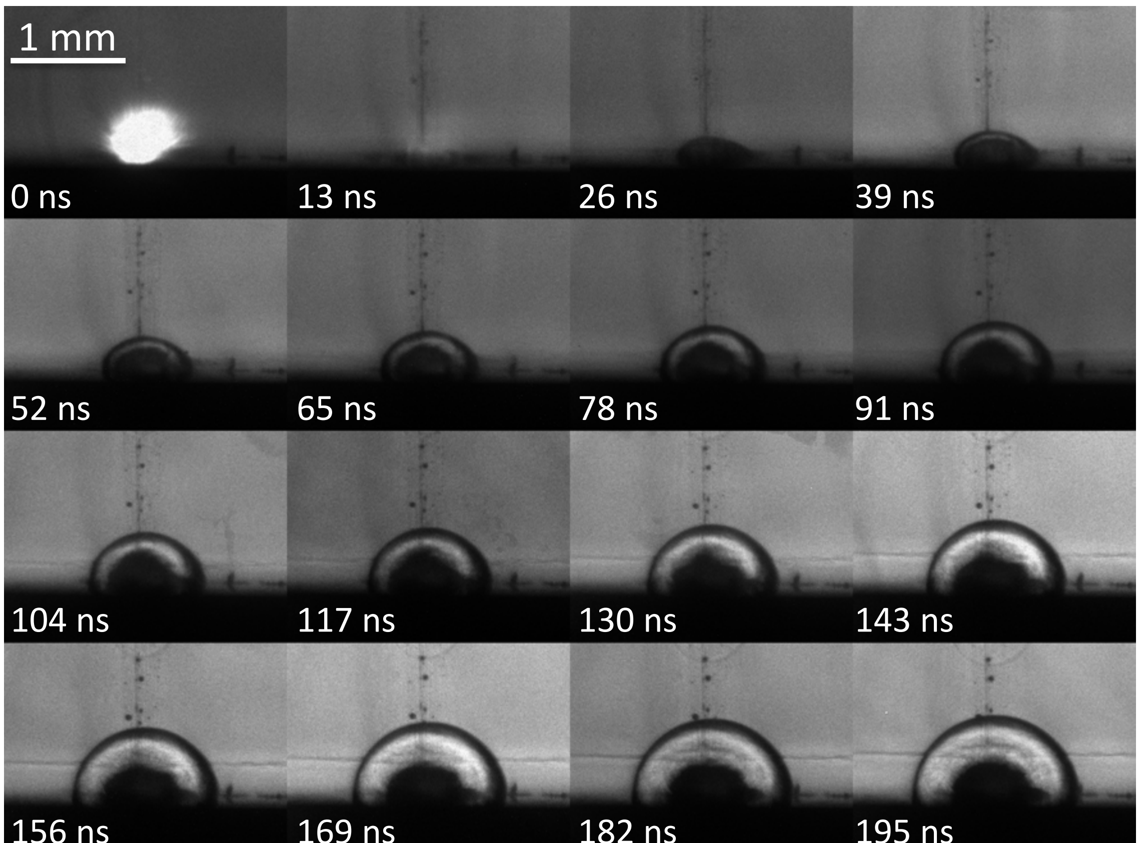

Shadowgraph imaging using a SIMX camera (16 iCCD, Gate 5ns).

Consistency with molecular dynamics ?

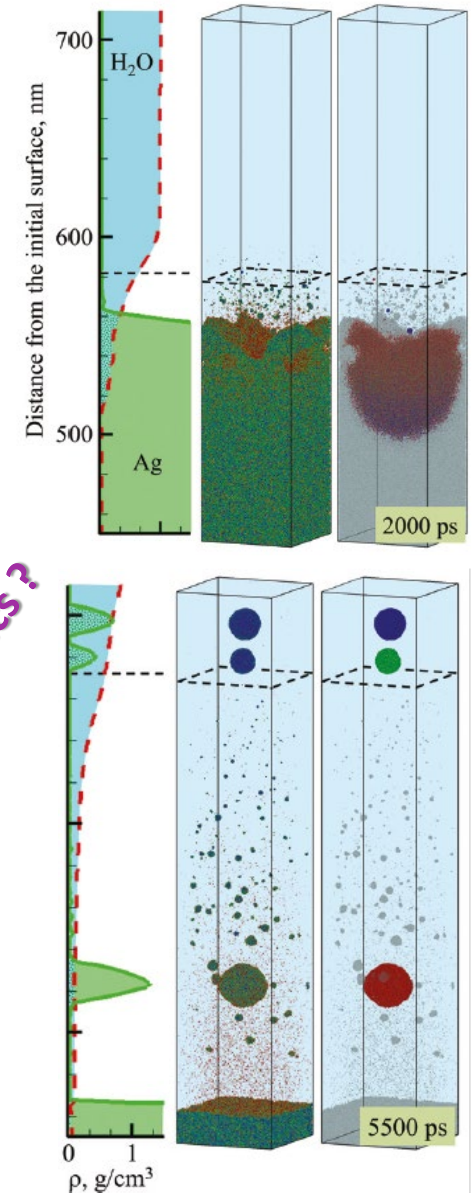

Cheng-Yu Shih et al., Nanoscale, 2018, 10, 6900

Plasma spectroscopy

- **Overview**
- **Temperatures**
- **LIF measurement**

Plasma spectroscopy : measurement of thermodynamic parameters

- **Plasma species and time evolution of the chemical composition**

    atomic / ionic / diatomic molecules

- **Plasma temperatures**

    diatomic molecules : $T_{rotational}$, $T_{vibrational}$
    Electronic temperature of atoms, ions molecules : T_{elec}
    (electrons (kinetics) : T_e)

- **Electron density (n_e):**

    Electronic field => Stark effects (broadening and shift)

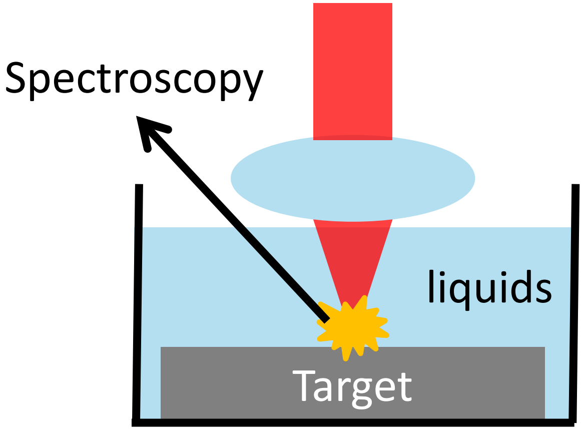

Plasma spectroscopy

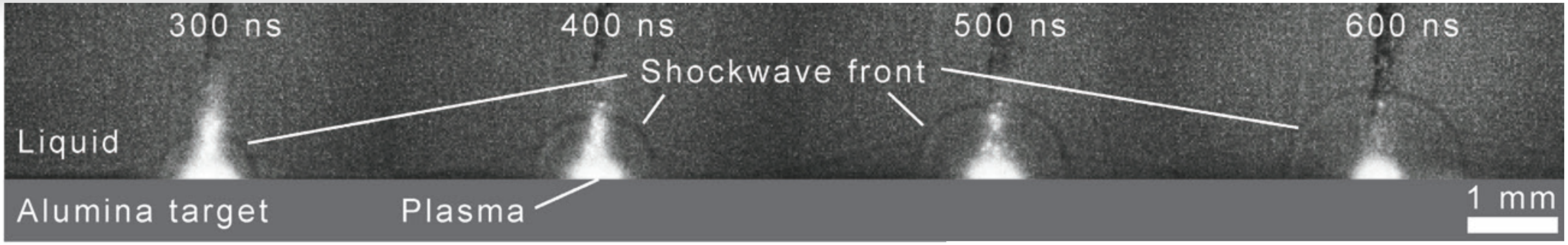

Shadowgraph imaging using an iCCD

5 ns pulses
10^{10} - 10^{12} W/cm^2

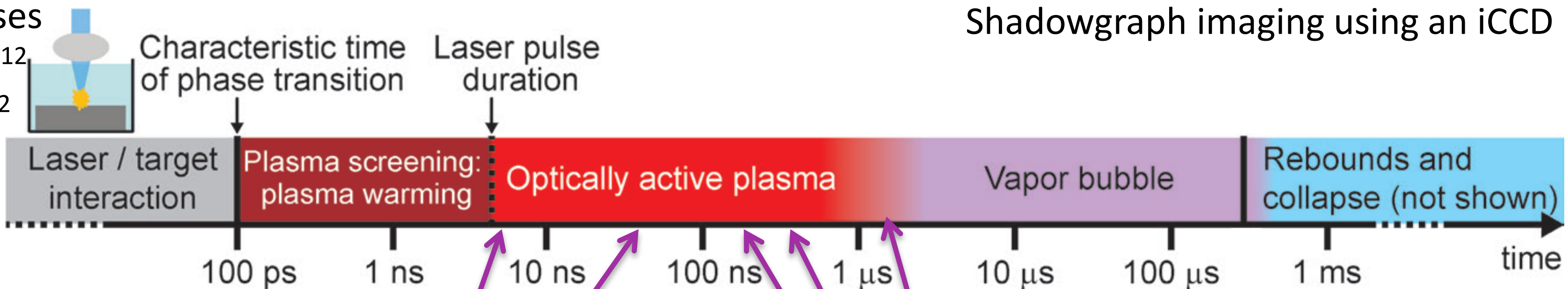

Carbon target -> C_2 swan band

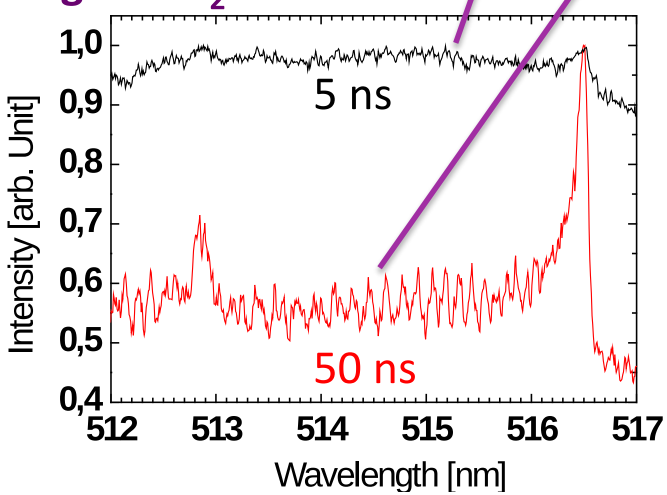

Al_2O_3 target -> AlO molecules

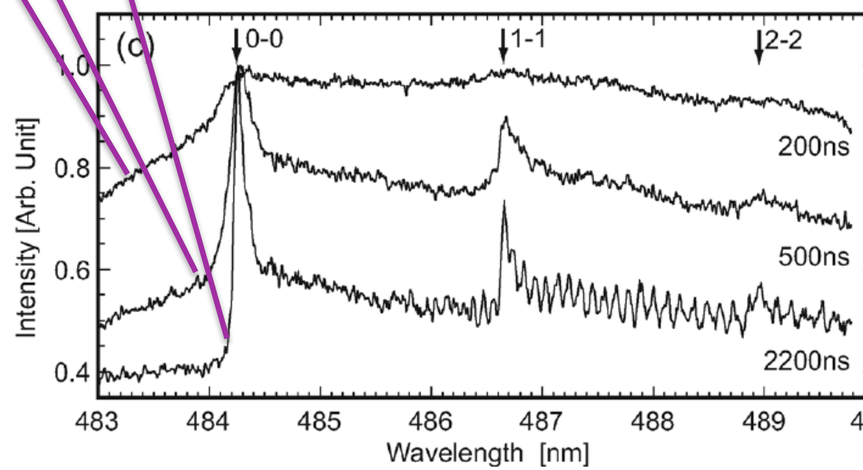

Molecules appear early (with respect to what is observed in gas or vacuum) -> problem for LIBS

Plasma spectroscopy: Electron density

BG : Background emission
Stark : Stark shift/broadening

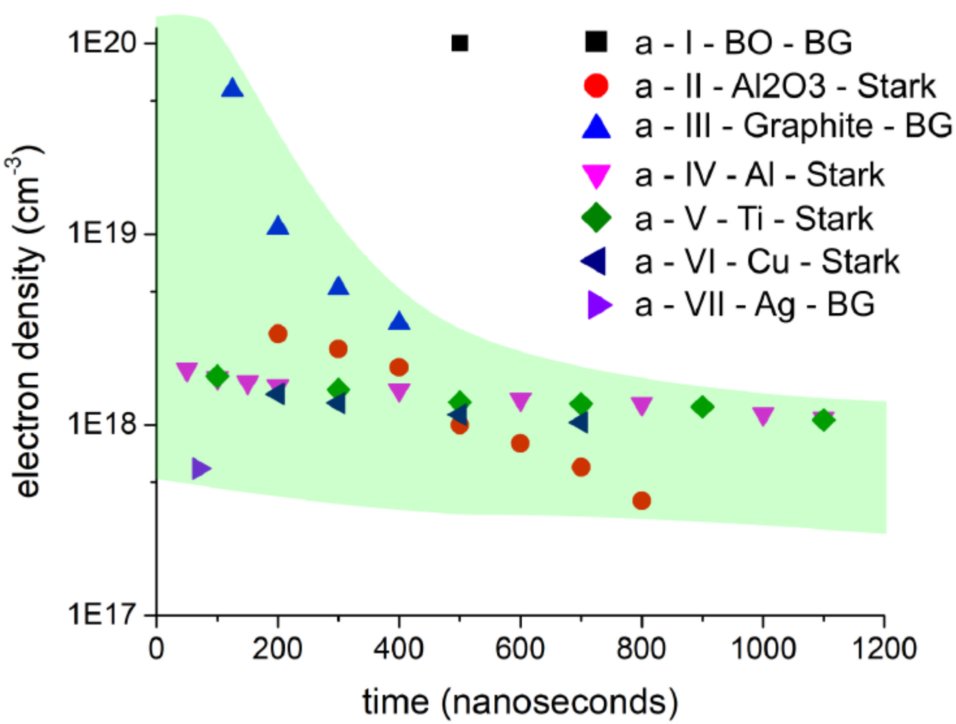

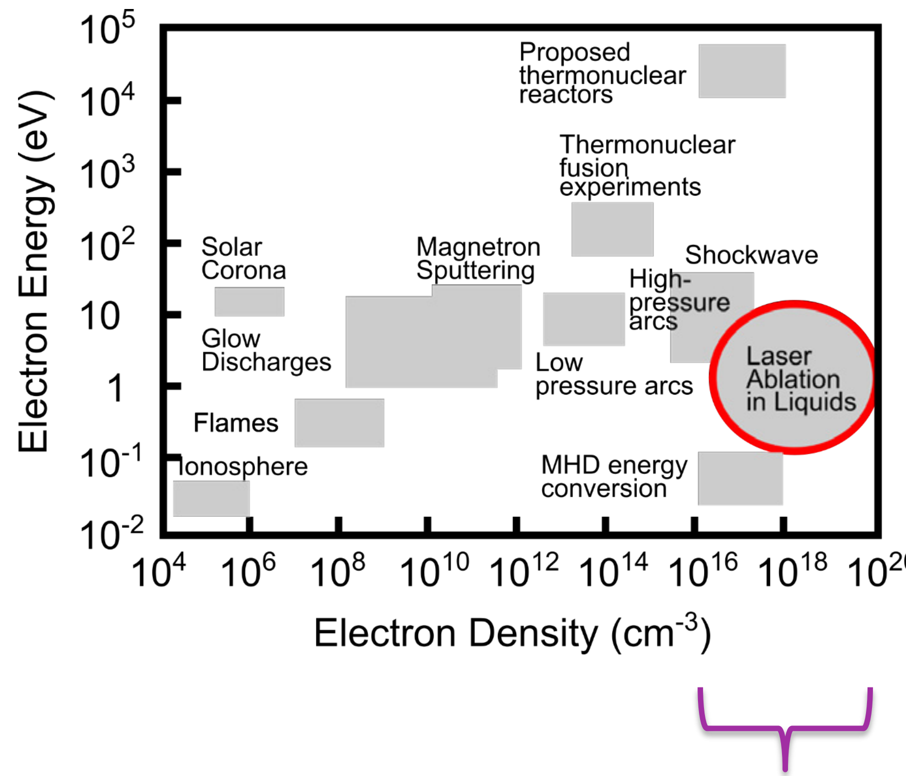

Here… good news for what concerns the local thermodynamic equilibrium <u>for the electronic states</u>

$$N_e \geqslant 6.5 \times 10^{16} \times \frac{g_{max}}{g_{min}} \left(\frac{\Delta E}{E_1^H}\right)^3 \left(\frac{kT_{elec}}{E_1^H}\right)^{0.5} \Phi_1 \left(\frac{\Delta E}{kT_{elec}}\right)$$

[Review] A. Kanitz et al., Plasma Sources Sci. Technol. (2019)

H. Drawin, Zeitschrift fur Physik, 1969, 228, 99.

Exemple on Al_2O_3 target

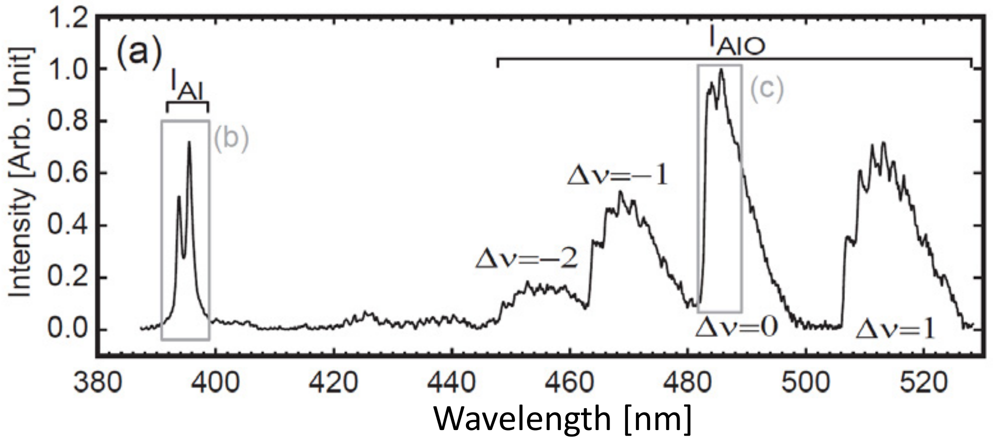

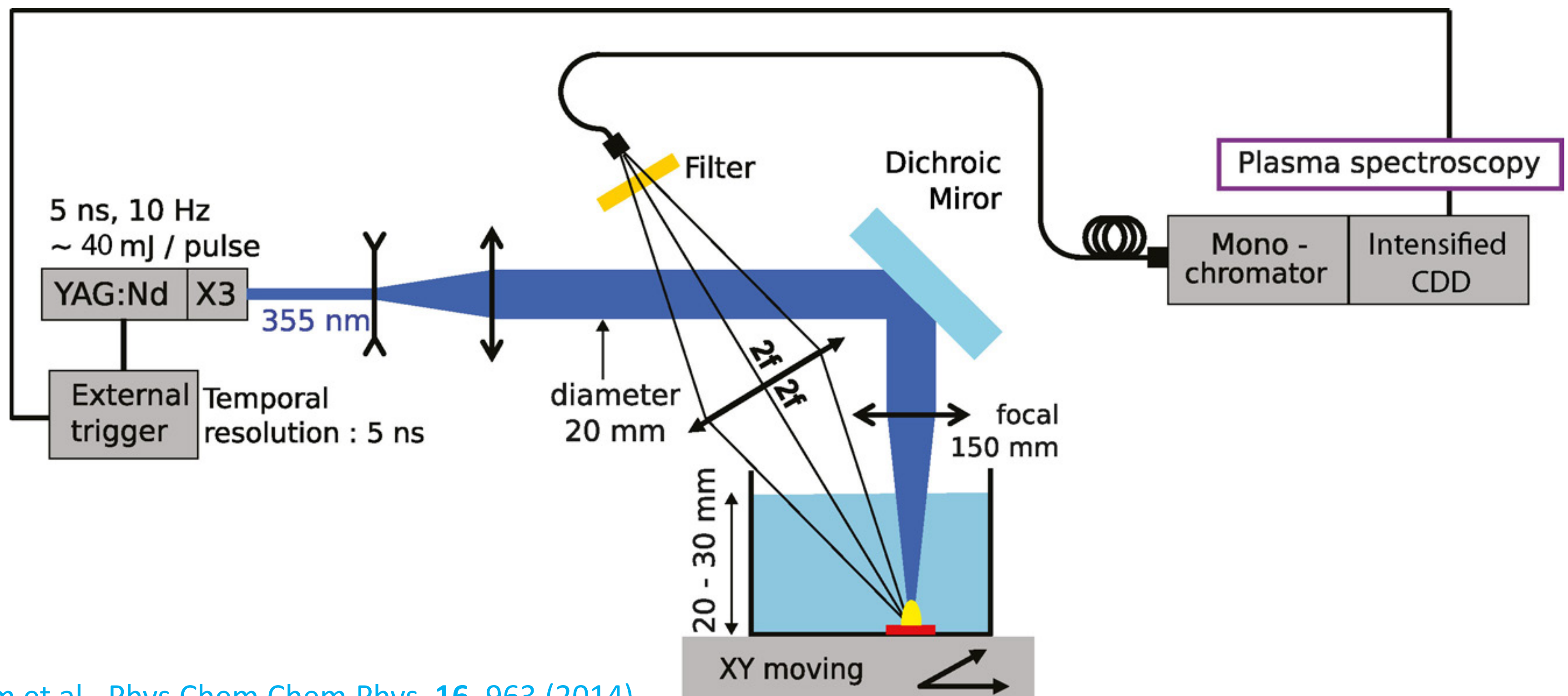

J. Lam et al., Phys.Chem.Chem.Phys. **16**, 963 (2014)

Plasma spectroscopy: Ro-vibrational spectroscopy

Temperatures:

- Atoms : T_{elec}
- Diatomic molecules : T_{elec} , T_{vib} , T_{rot}

canonical ensemble

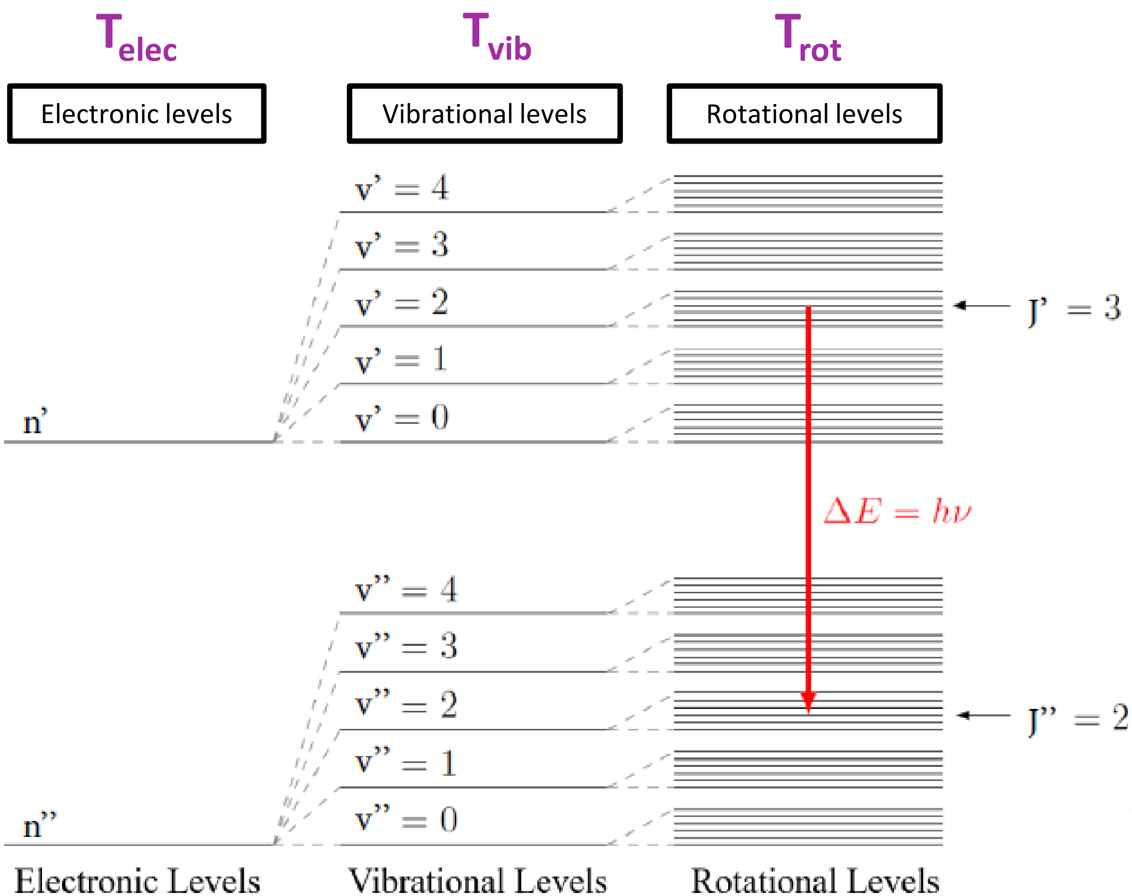

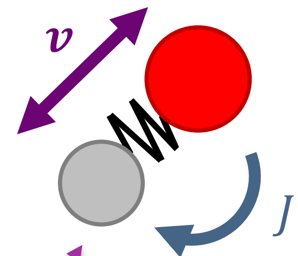

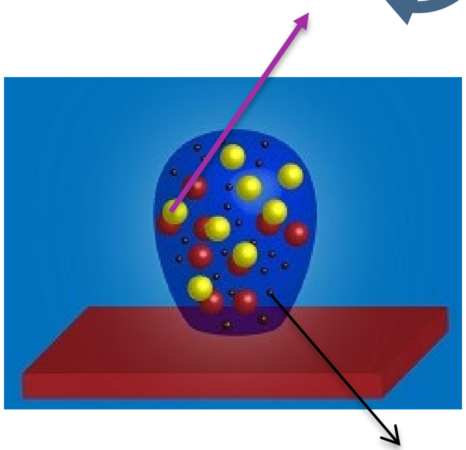

Electron : Kinetic temperature T_e

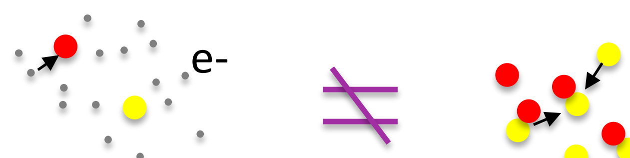

Plasma spectroscopy: Ro-vibrational spectroscopy

$$E = T_n + G_n(v) + F_v(J)$$

... but $F_v(J)$ Depend on the Hund's case ($\vec{S}$, $\vec{L}$, $\vec{N}$ and their projection)

Istvan Kovacs (1969)

$$G_n(v) = w_e\left(v+\frac{1}{2}\right) - w_e x_e\left(v+\frac{1}{2}\right)^2 + w_e y_e\left(v+\frac{1}{2}\right)^3 + \ldots \quad (cm^{-1}).$$

$$F_v(J) = B_v \cdot J(J+1) - D_v \cdot \Big(J(J+1)\Big)^2 + \ldots + H(J,K,S,\Lambda,\Sigma\ldots) \quad (cm^{-1})$$

Tabulated

$$I^{n',v',J'}_{n'',v'',J''} = hc \cdot \cancel{\bar{\nu}^{n',v',J'}_{n'',v'',J''}} \cdot A^{n',v',J'}_{n'',v'',J''} \cdot N_{n',v',J'} \qquad (W \cdot m^{-3}).$$

Intensity

band strength

Probability of spontaneous transition(s^{-1}) $A^{n',v',J'}_{n'',v'',J''} = A^{n',v'}_{n'',v''} \cdot A^{J'}_{J''}$

Einstein Coefficient $A^{n',v'}_{n'',v''} = \dfrac{1}{4\pi\varepsilon_0}\dfrac{64\pi^4}{3h(2-\delta_{0,\Lambda'})(2S'+1)} \cdot (100 \cdot \bar{\nu}^{n',v',J'}_{n'',v'',J''})^3 \cdot S^{n',v'}_{n'',v''} \cdot (a_0 e)^2$

$$A^{J'}_{J''} = \frac{S^{J'}_{J''}}{2J'+1}$$

Höln-London's coefficient

$$\boxed{\sum_{sub-rot\ \ states} S^{J'}_{J''} = (2-\delta_{0,\Lambda'})(2S'+1)(2J'+1)}$$

Normalisation, Istvan Kovacs (1969)

$$N_{n',v',J'} = N_{n'} \cdot \frac{1}{2} \cdot (2J'+1) \cdot \frac{exp\left(-\frac{hc \cdot F_{v'}(J')}{k_B \cdot T_{rot}}\right)}{Q_{rot_{n',v'}}(T_{rot})} \cdot \frac{exp\left(-\frac{hc \cdot G_{n'}(v')}{k_B \cdot T_{vib}}\right)}{Q_{vib_{n'}}(T_{vib})}$$

Population density of the **excited state**

$AlO(B^2\Sigma^+) \longrightarrow AlO(X^2\Sigma^+)$

visible light (~ 500 nm)

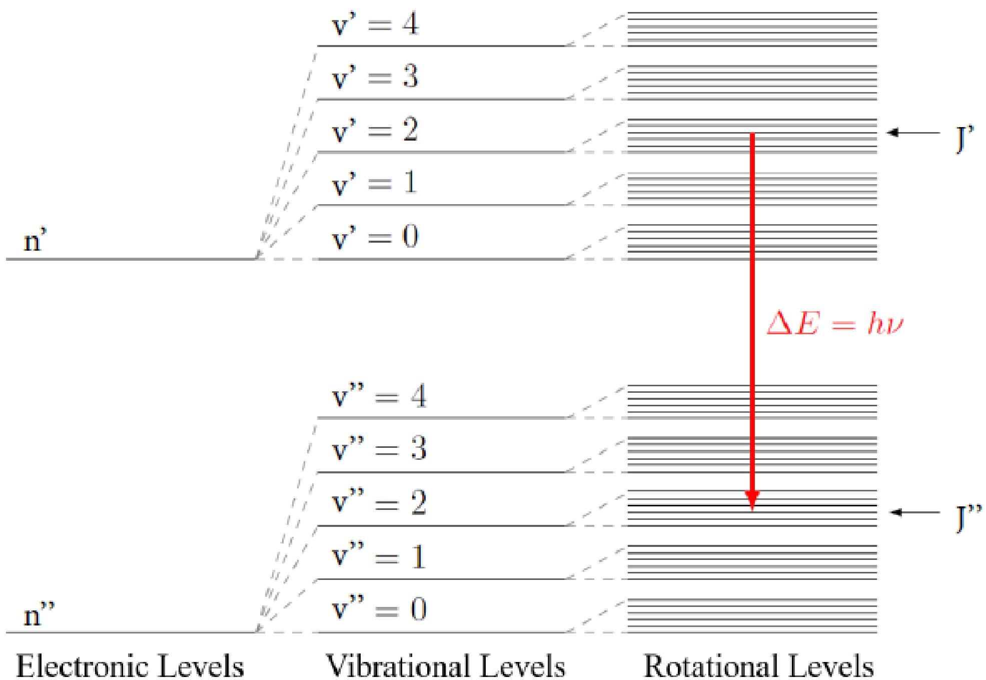

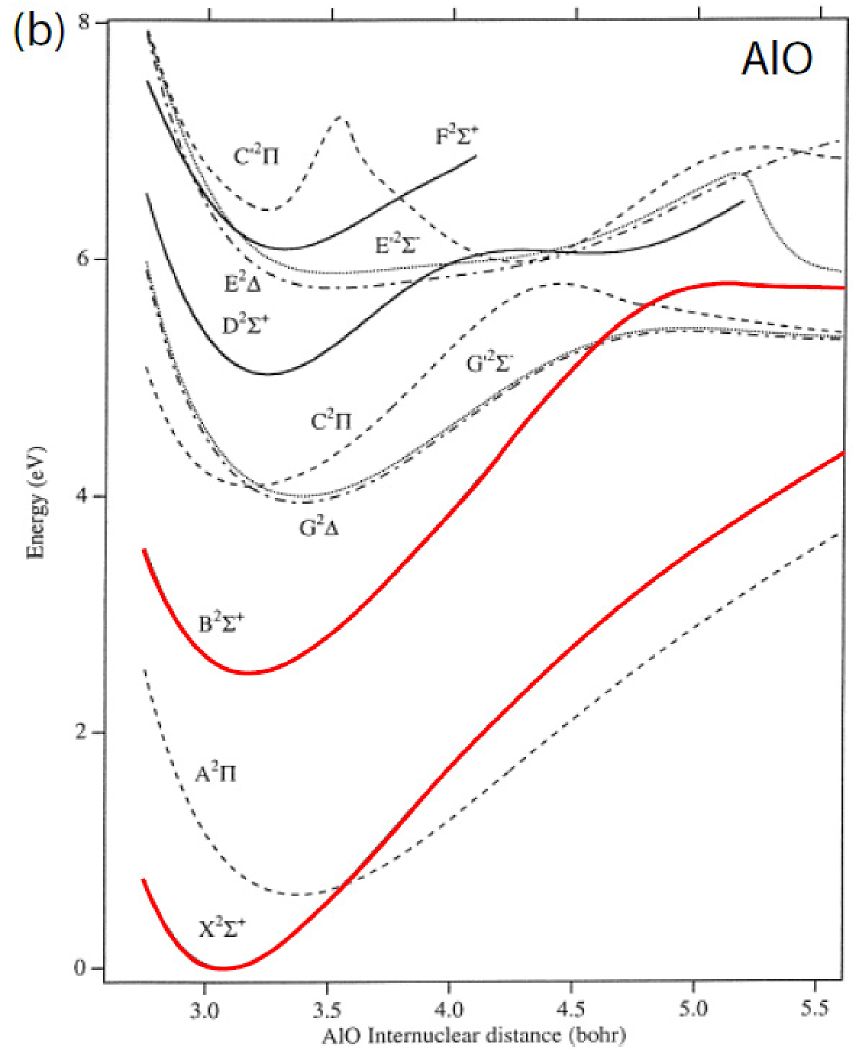

Plasma spectroscopy: Temperatures

Atomic AlO emission

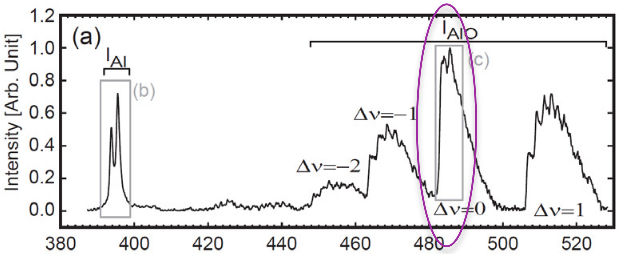

AlO molecules emission

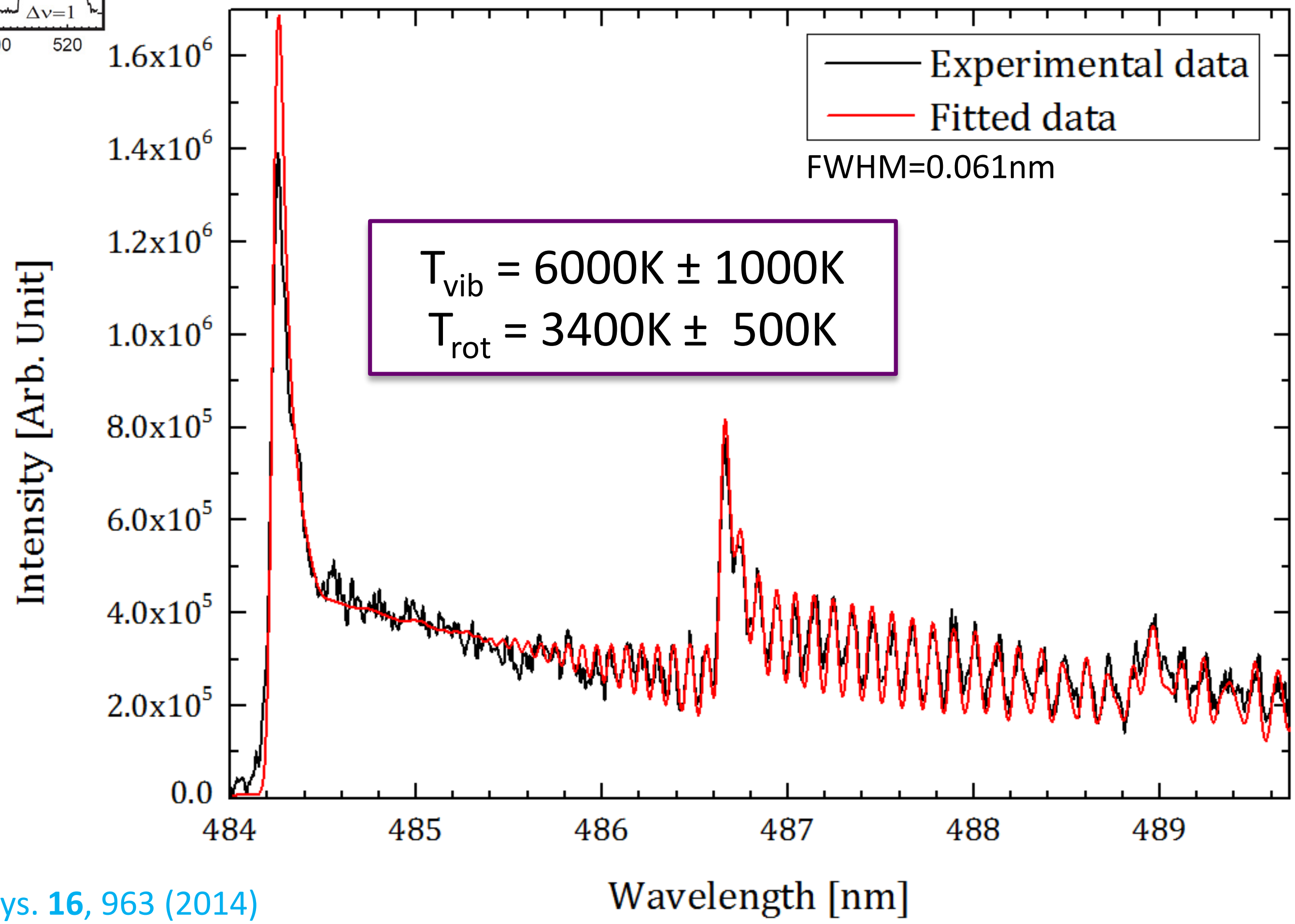

J. Lam et al., Phys.Chem.Chem.Phys. **16**, 963 (2014)

Plasma spectroscopy: Temperatures

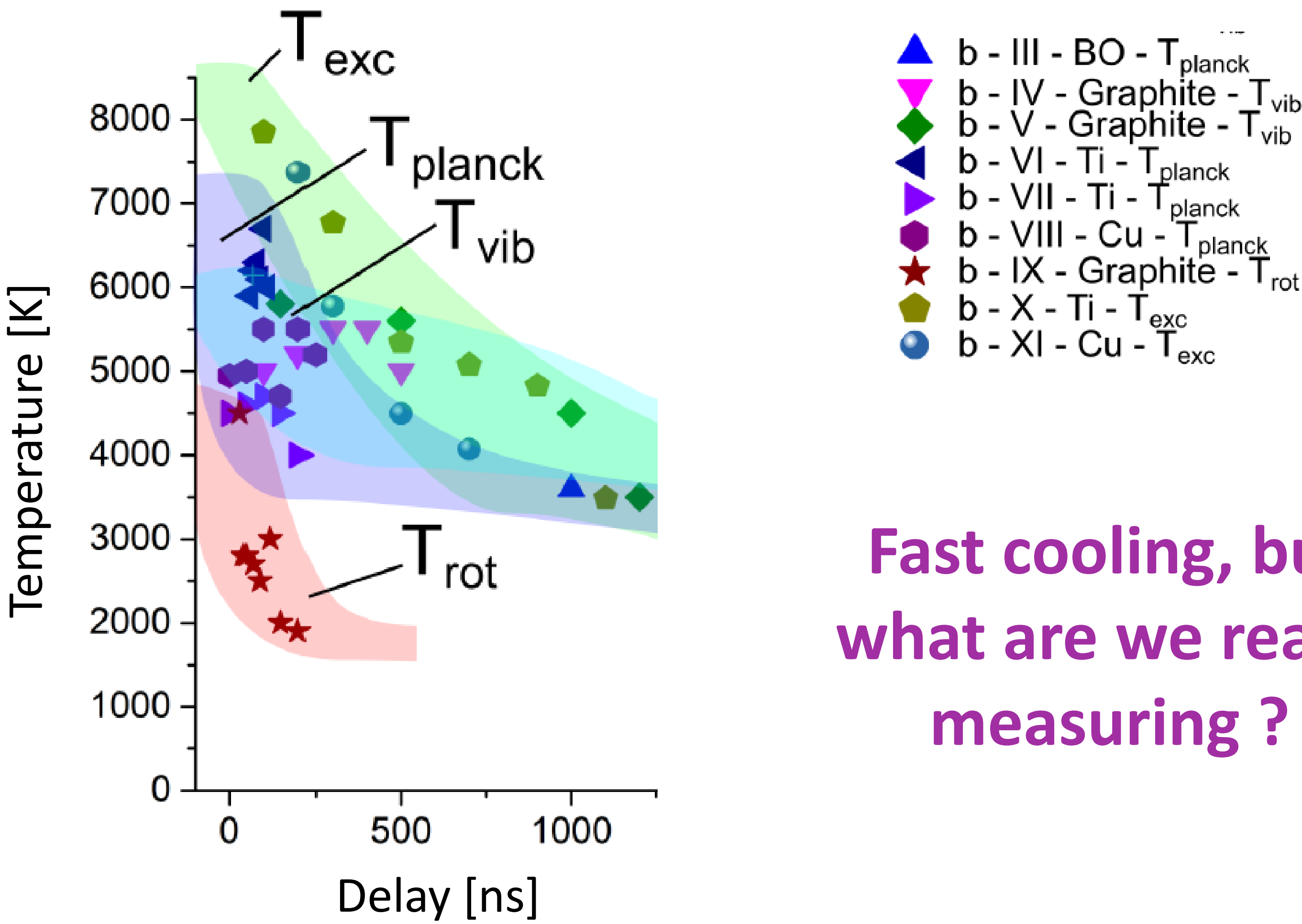

Fast cooling, but what are we really measuring ?

[Review] A. Kanitz et al., Plasma Sources Sci. Technol. (2019)

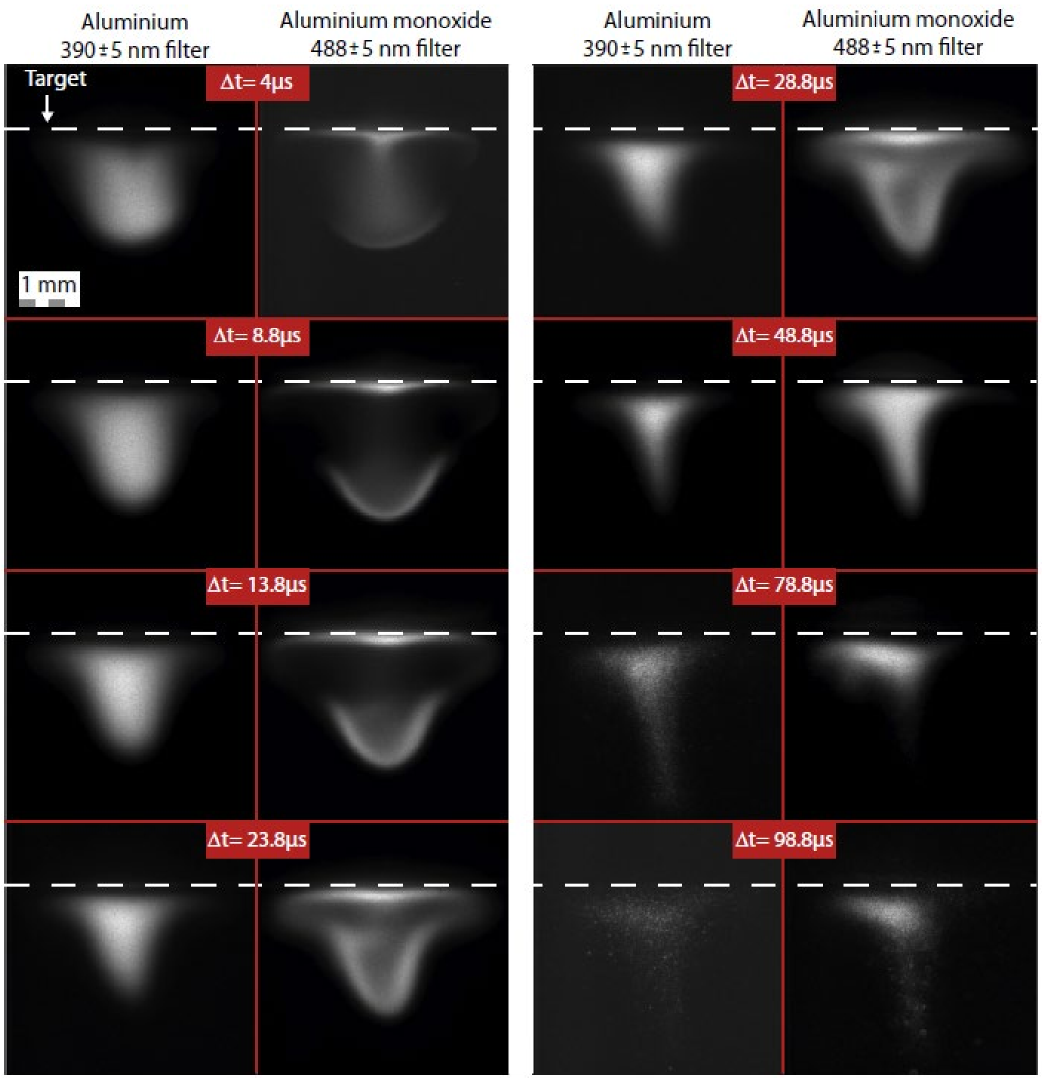

What are we really measuring ?

Emission from "newly" produced molecules ?

J. Lam et al., Spectrochimica Acta Part B 101 (2014) 86–92

Light-induced Fluorescence (LIF)

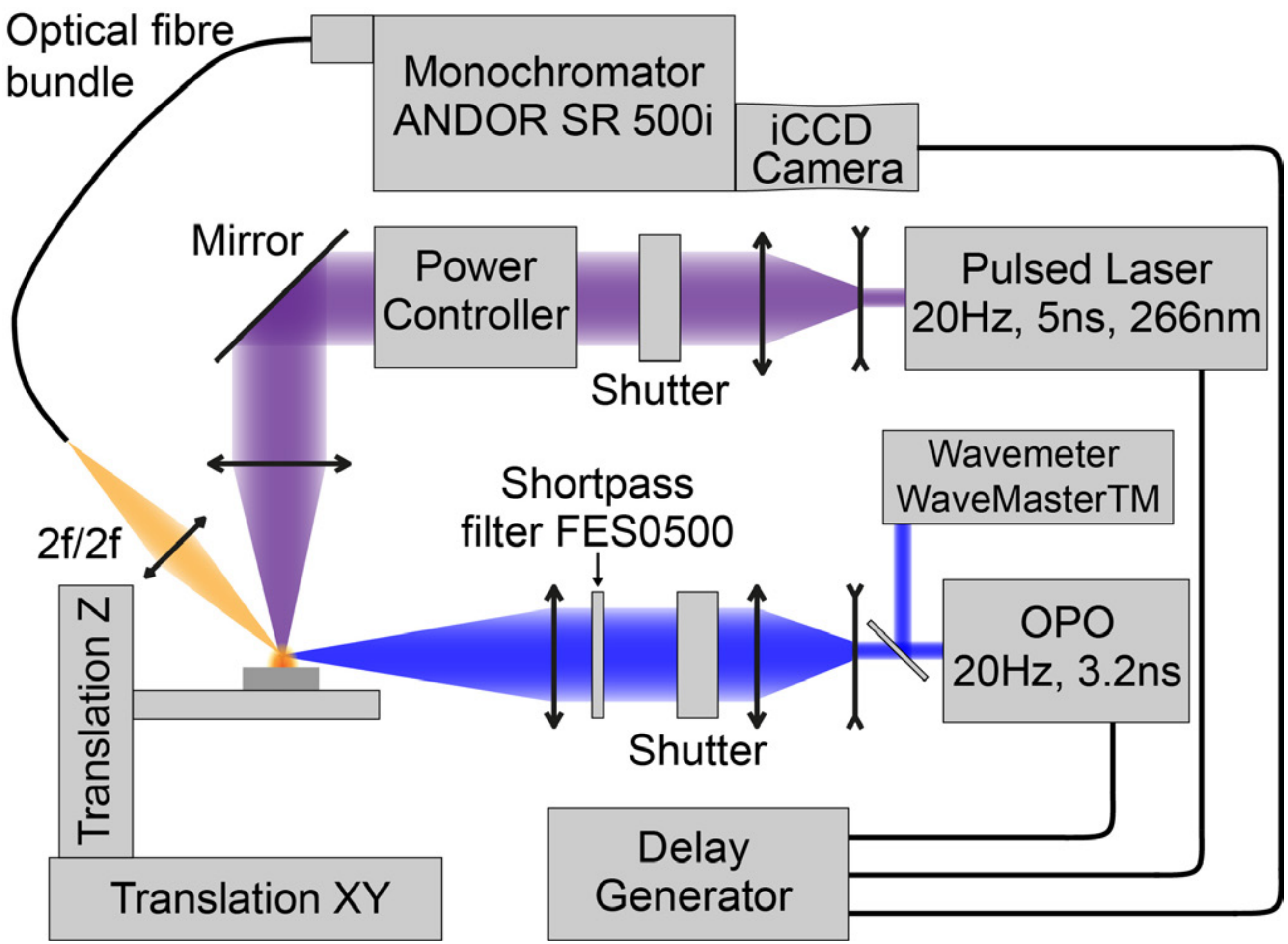

A. Chemin et al., Spectrochimica Acta Part B: Atomic Spectroscopy 205 (2023) 106685

Light-induced Fluorescence (LIF)

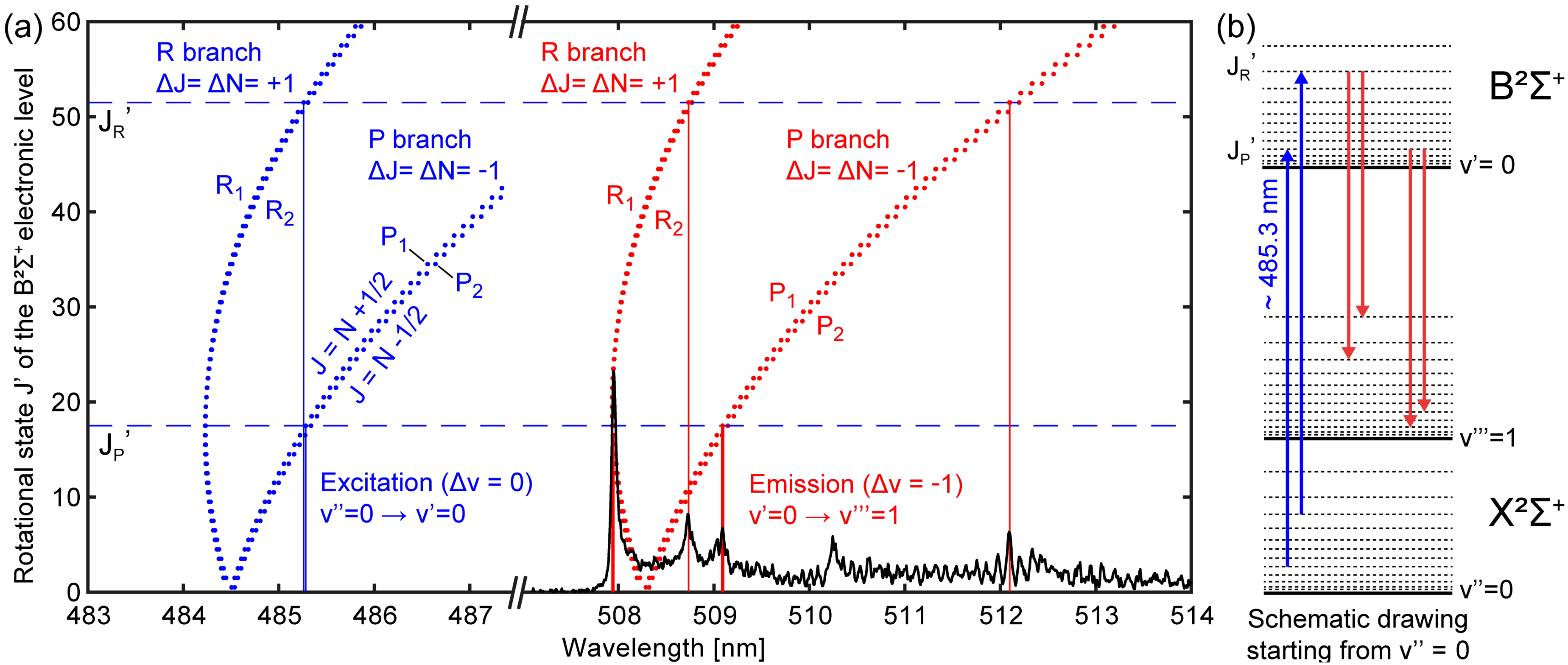

A. Chemin et al., Spectrochimica Acta Part B: Atomic Spectroscopy 205 (2023) 106685

Light-induced Fluorescence (LIF)

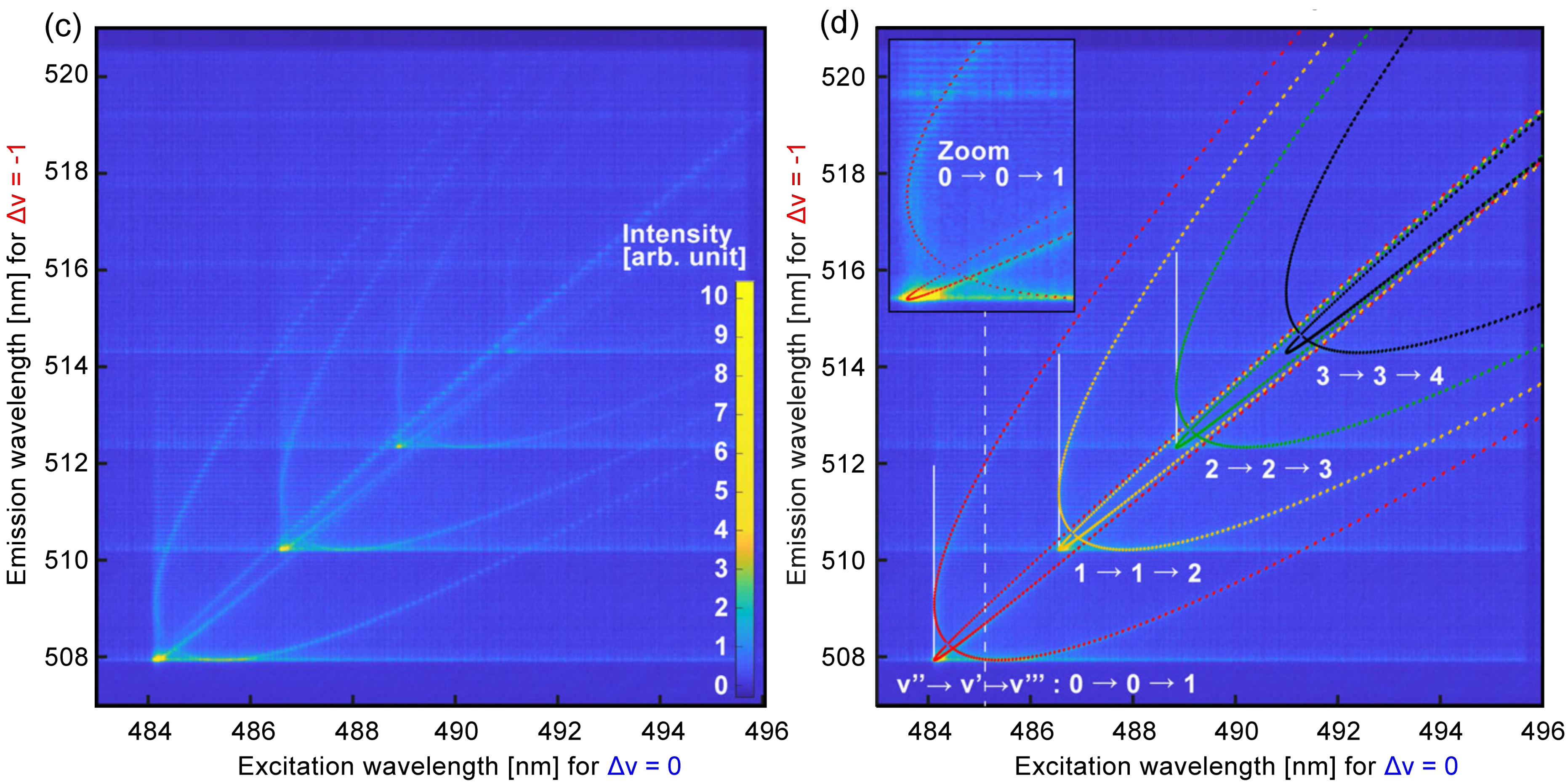

A. Chemin et al., Spectrochimica Acta Part B: Atomic Spectroscopy 205 (2023) 106685

Light-induced Fluorescence (LIF)

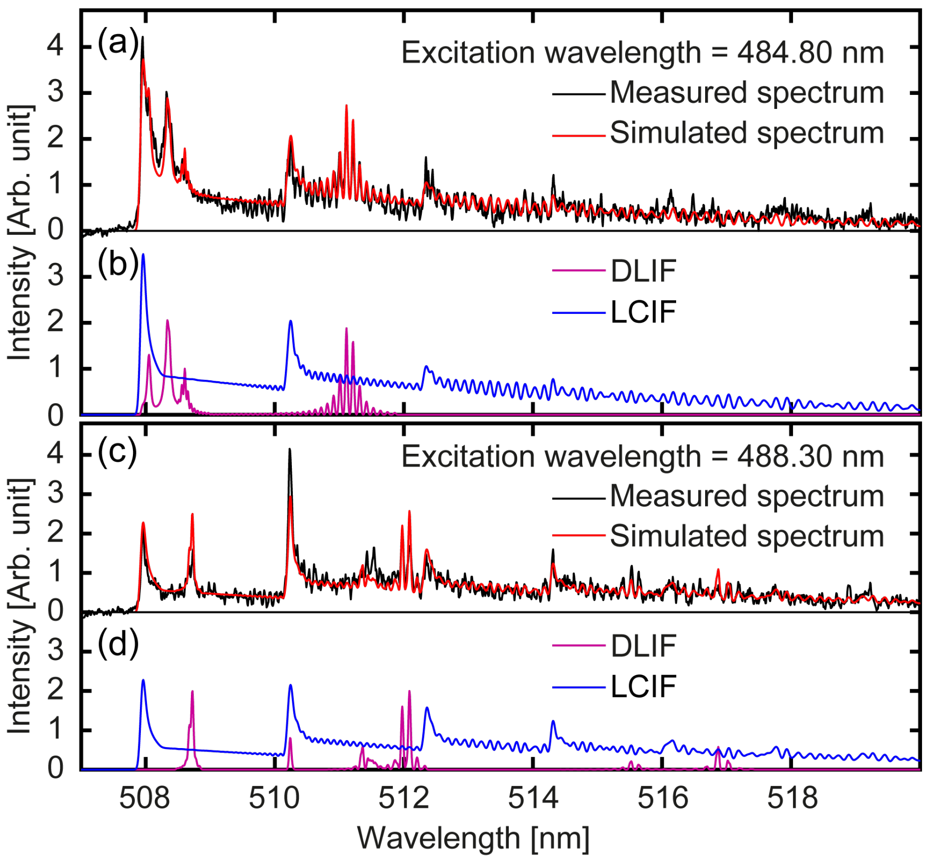

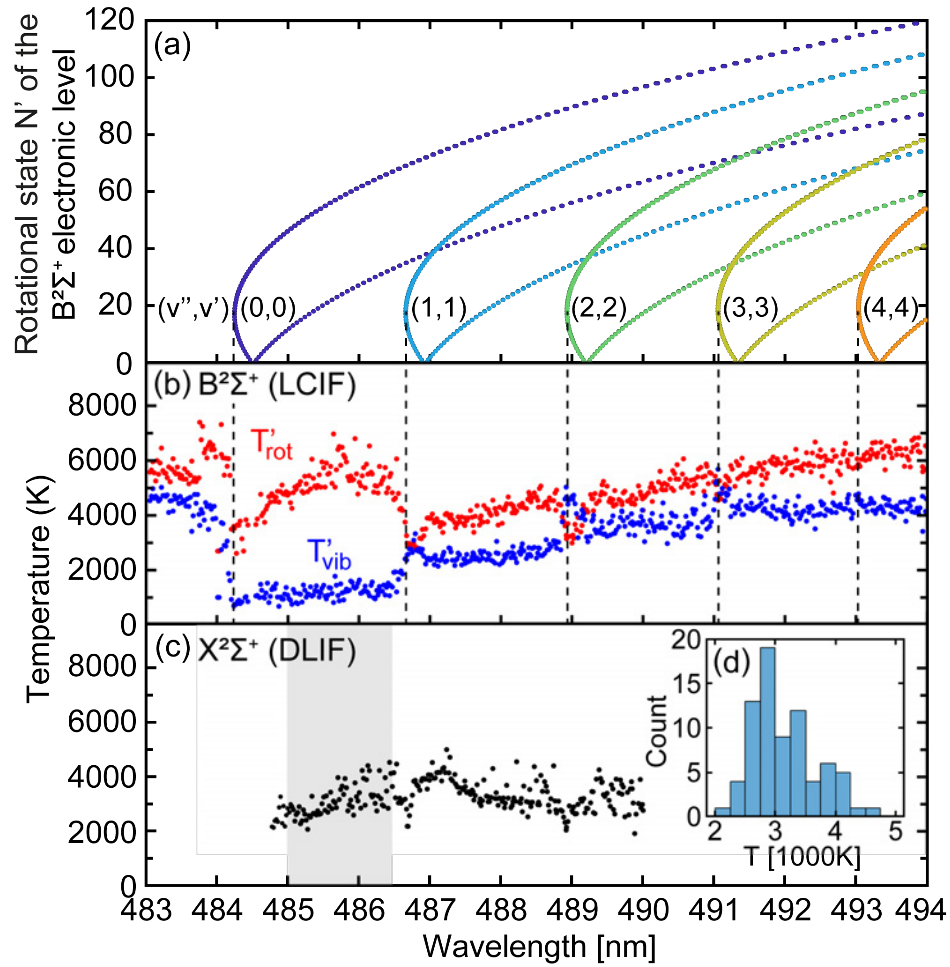

Collisionally induced fluorescence contribution in blue (LCIF)

Direct fluorescence contribution in magenta (DLIF)

A. Chemin et al., Spectrochimica Acta Part B: Atomic Spectroscopy 205 (2023) 106685

Light-induced Fluorescence (LIF)

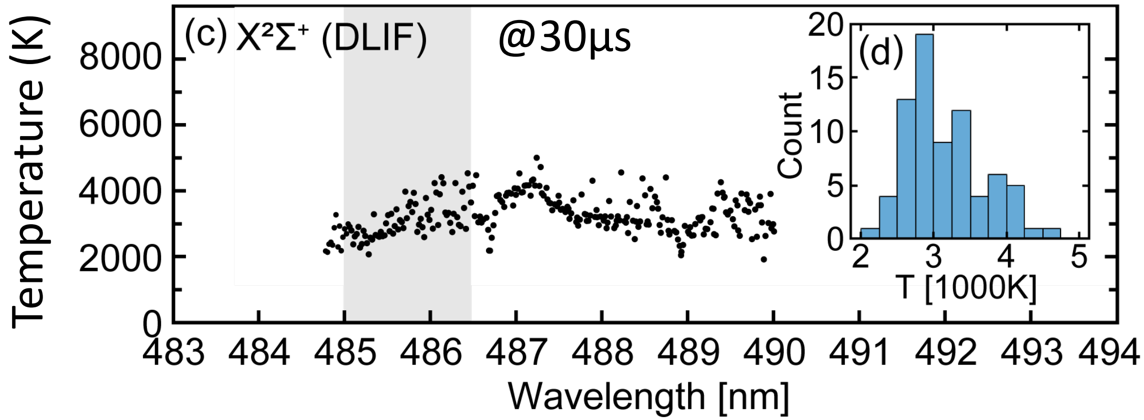

LIF

@30µs : $\boldsymbol{T_{X^2\Sigma^+} = 3150\ \mathrm{K}}$ (SD = 552 K)
Temperature interval for a confidence level of 70% (two-sided) is ±67 K.

@5µs : $\boldsymbol{T_{X^2\Sigma^+} = 3700\ \mathrm{K}}$ (SD = 5302 K)
Temperature interval for a confidence level of 70% (two-sided) is ±64 K.

Vs.

Plasma emission

$T^{rot}_{B^2\Sigma^+} = 3130 \pm 100$ K (70%).

$T^{rot}_{B^2\Sigma^+} = 3850 \pm 100$ K (70%)

A. Chemin et al., Spectrochimica Acta Part B: Atomic Spectroscopy 205 (2023) 106685

Bubble dynamics

- **Imaging of laser-generated bubbles in solvents of low viscosity**
- **Rayleigh-Plesset equation**
- **Gilmore model**
- **Bubbles in highly viscous liquids**

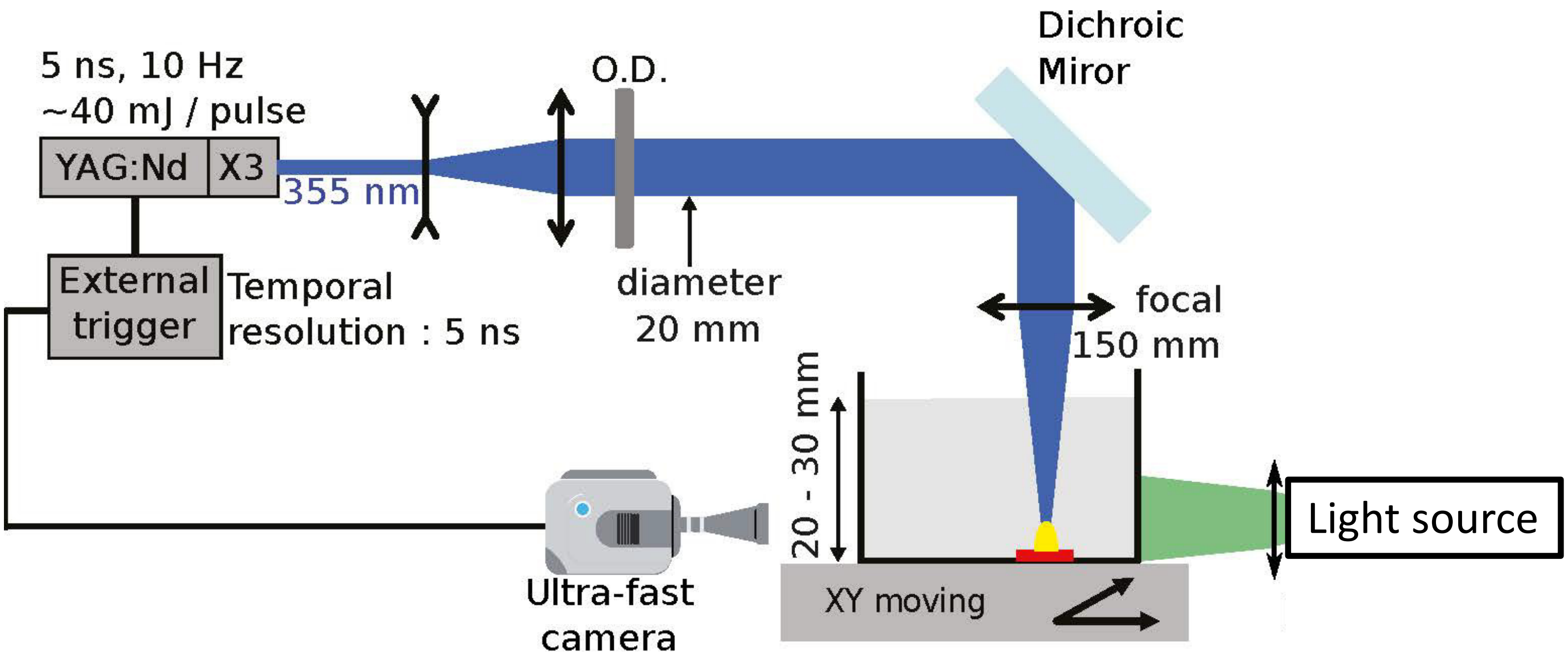

Camera Phantom v711 from
Vision Research
Zoom 6000 from Navitar
Frame rate 210000 fps

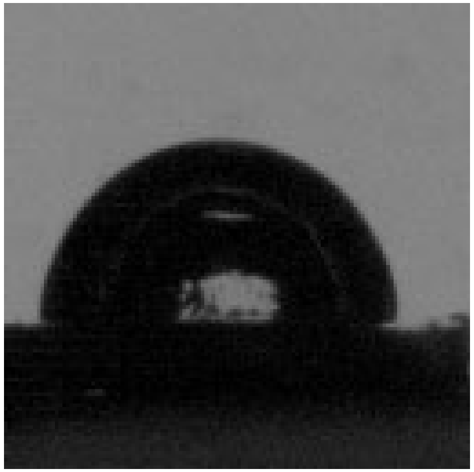

Let me focus on the first oscillation.
The bubble radius appears symmetric
with respect to time !

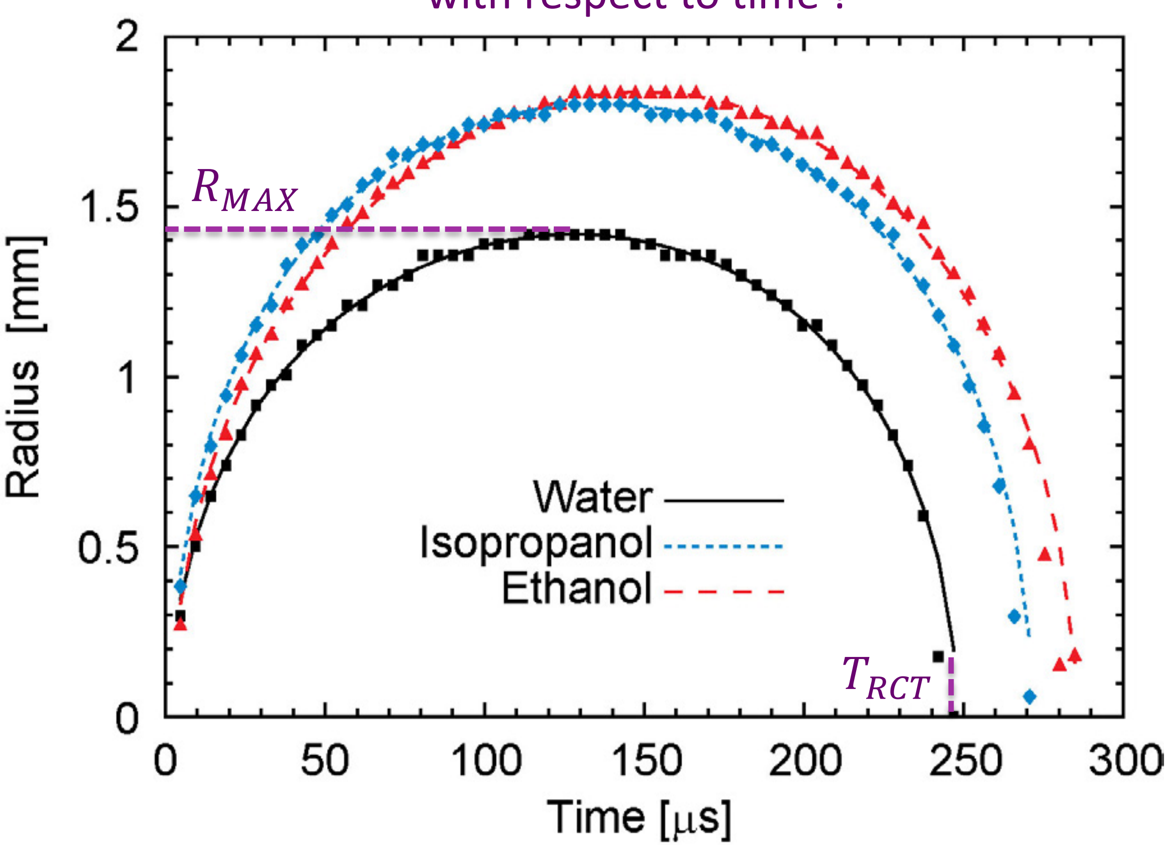

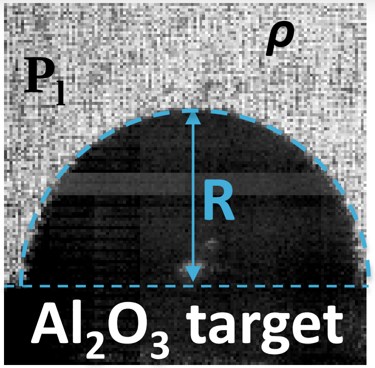

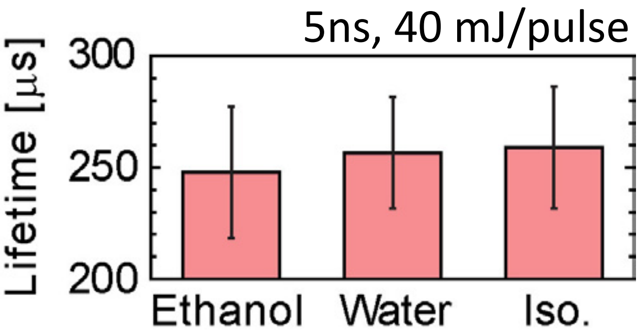

Rayleigh collapse time:

$$T_{RCT} = 1{,}83\, R_{MAX} \sqrt{\frac{\rho}{P_l}}$$

J. Lam *et al.*, Appl. Phys. Lett. **108**, 074104 (2016)

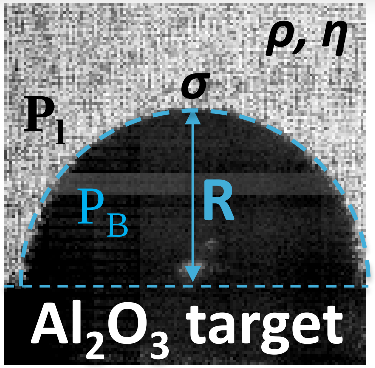

σ fluid surface tension
ρ liquid mass density
η dynamic viscosity

Rayleigh-Plesset (RP) equation
Derive from Navier–Stokes equations in spherical coordinates, assuming a Newtonian fluid, **incompressible**

$$R\ddot{R} + \frac{3}{2}\dot{R}^2 = \frac{1}{\rho}\left[P_B(t) - P_l - \frac{2\sigma}{R} - \frac{4\eta\dot{R}}{R}\right]$$

Relative contribution of each term :

R ≈1 mm, t ≈300 µs, $\sigma_w \approx 0{,}1$ N/m , $\rho_w \approx 1$ g/cm^3, $\eta_w \approx 10^{-3}$ Pa.s

Weber number $\mathcal{W}e = \rho\dot{R}^2 R/\sigma \simeq 1\times 10^2$

Reynolds number $\mathcal{R}e = \rho\dot{R}R/\eta \simeq 3\times 10^3$

The surface motion of the bubble is driven by inertial forces

Simplified Rayleigh-Plesset (RP) equation for **purely inertial dynamics**

$$\rho(R\ddot{R} + \frac{3}{2}\dot{R}^2) = P_B(t) - P_l$$

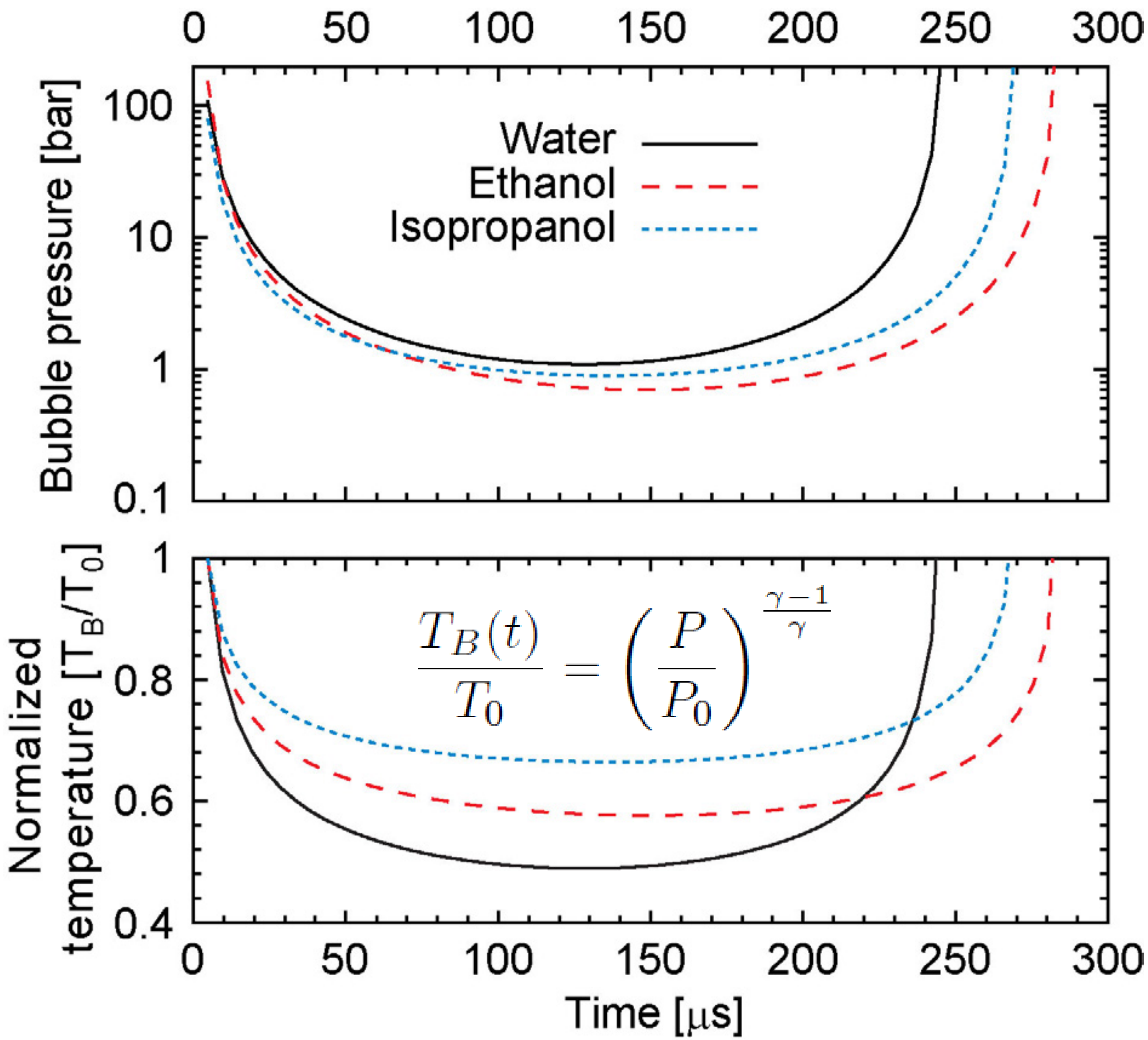
Bubble pressure [bar]
100
10
1
0.1
0
50
100
150
200
250
300
Water
Ethanol
Isopropanol
Normalized temperature [T_B/T_0]
1
0.8
0.6
0.4
$$\frac{T_B(t)}{T_0} = \left(\frac{P}{P_0}\right)^{\frac{\gamma-1}{\gamma}}$$
Time [µs]

Isentropic process !

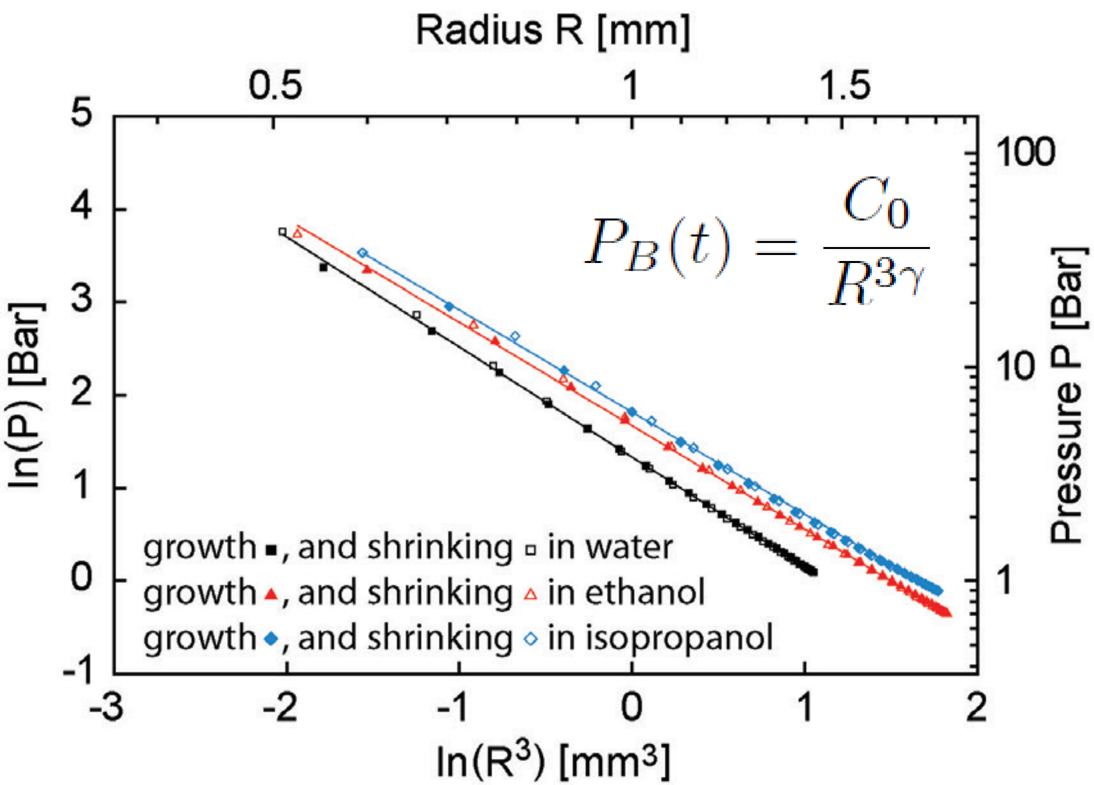

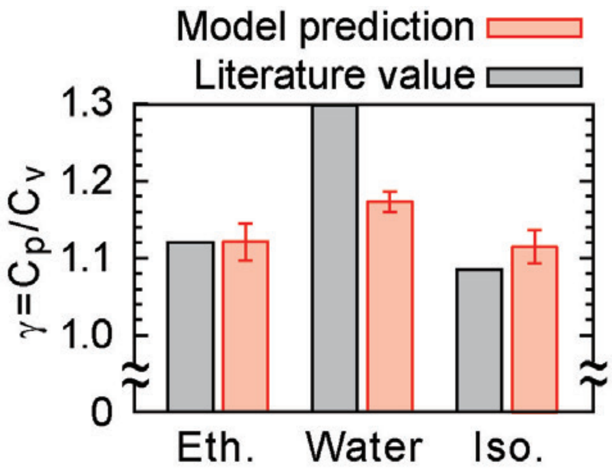

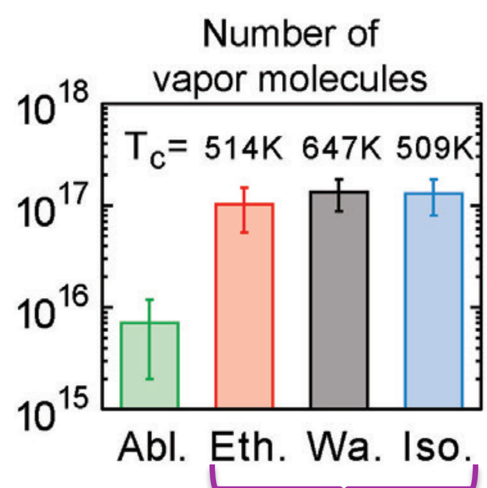

Adiabatic ?

R ≈1 mm, h ≈ 100 W/m²/K, T_c ≈ 650 K

$\Phi = h\Delta T(\pi R^2 + 2\pi R^2) \approx 0{,}33$ W

300 µs → 0,1 mJ

Vapor mainly composed of solvent molecules (25% pulse energy)

But the Rayleigh-Plesset (RP) model can't explain the damping of the bubble oscillation … we need to account the compressibility ➔ Gilmore model

Computes: $R(t)$, $P_B(t)$ and the pressure distribution in the surrounding liquid.

Considers: liquid compressibility, viscosity and surface tension.

Assumes: a constant gas content of the bubble, neglecting evaporation, condensation, gas diffusion through the bubble wall, and heat conduction.
Gas content variation during the collapse is arbitrary added

State equation: Tait's equation

$$\frac{P+B}{p_\infty+B}=\left(\frac{\rho}{\rho_0}\right)^n$$

Water: B = 314 MPa, n=7

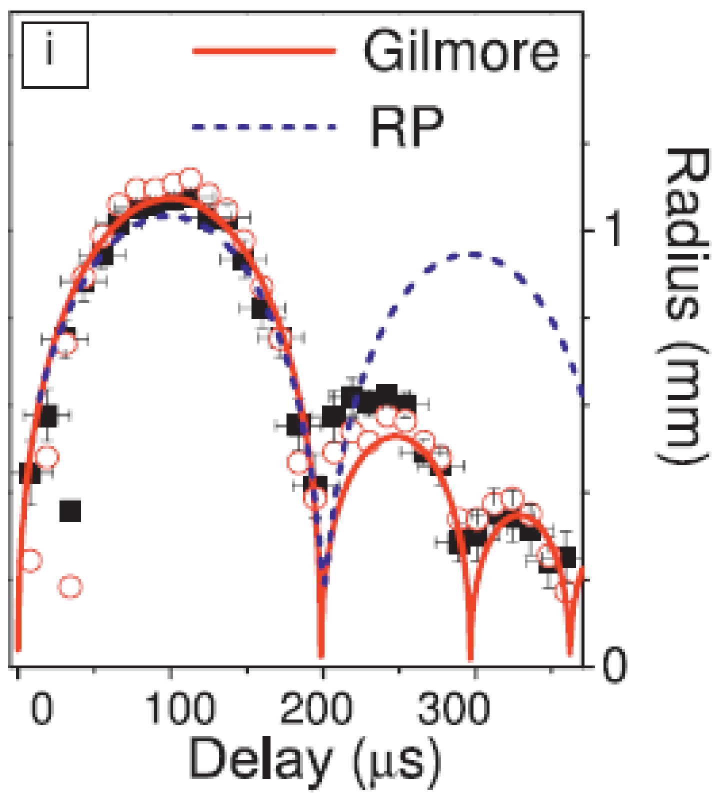

S. Barcikowski et al., MRS BULLETIN 44, 382 (2019)

A. Vogel et al., J. Acoust. Soc. Am. 100, 148 (1996).

But the <u>Rayleigh-Plesset</u> (RP) model can't explain the damping of the bubble oscillation …
we need to account the compressibility ➔ <u>Gilmore model</u>

$$\dot{U}=\left[-\frac{3}{2}\left(1-\frac{U}{3C}\right)U^2+\left(1+\frac{U}{C}\right)H+\frac{U}{C}\left(1-\frac{U}{C}\right)R\frac{dH}{dR}\right]\cdot\left[R\left(1-\frac{U}{C}\right)\right]^{-1}$$

R bubble radius, *U=dR/dt* is the bubble wall velocity,
C speed of sound in the liquid at the bubble wall,
H enthalpy difference between the liquid at pressure *P*(*R*) at the bubble wall and at hydrostatic pressure p_∞

$$H=\int_{p_\infty}^{P(R)}\frac{dp}{\rho}$$

p and ρ are the pressure and the density within the liquid

The pressure *P* at the bubble wall is given by

$$P=\left(p_\infty+\frac{2\sigma}{R_n}\right)\left(\frac{R_n}{R}\right)^{3\kappa}-\frac{2\sigma}{R}-\frac{4\mu}{R}U$$

κ the ratio of the specific heat
P is uniform in the bubble.
R_n equilibrium radius (P = P_{hydro})
R_n "measure" of the gas content

Assuming Tait's equation ➔

$$C=(c_0^2+(n-1)H)^{1/2},$$

$$H=\frac{n(p_\infty+B)}{(n-1)\rho_0}\left[\left(\frac{P+B}{p_\infty+B}\right)^{(n-1)/n}-1\right]$$

A. Vogel et al., J. Acoust. Soc. Am. 100, 148 (1996).

Ablation in viscous liquids : poly-*alpha*-olefin (PAO)

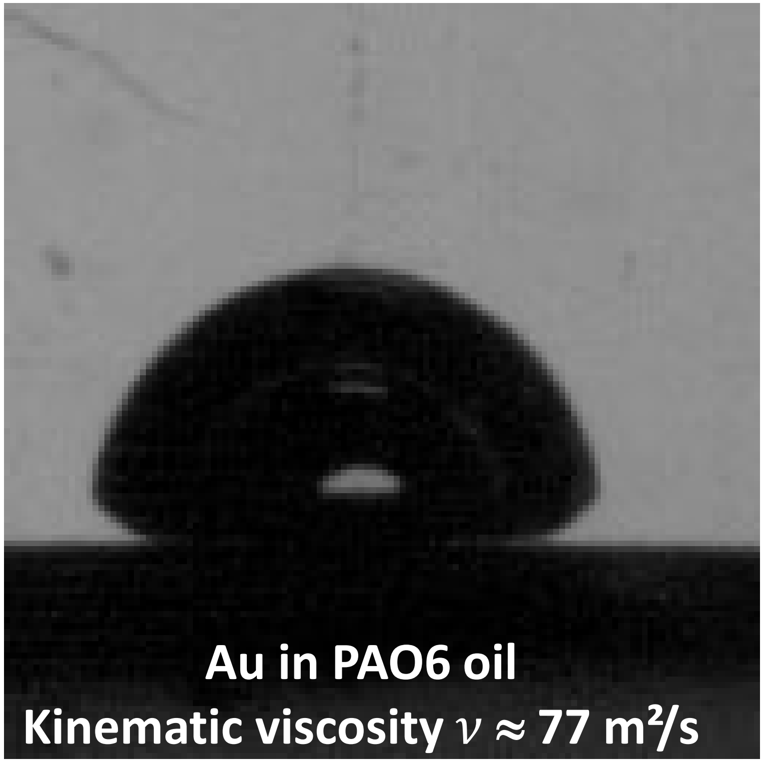

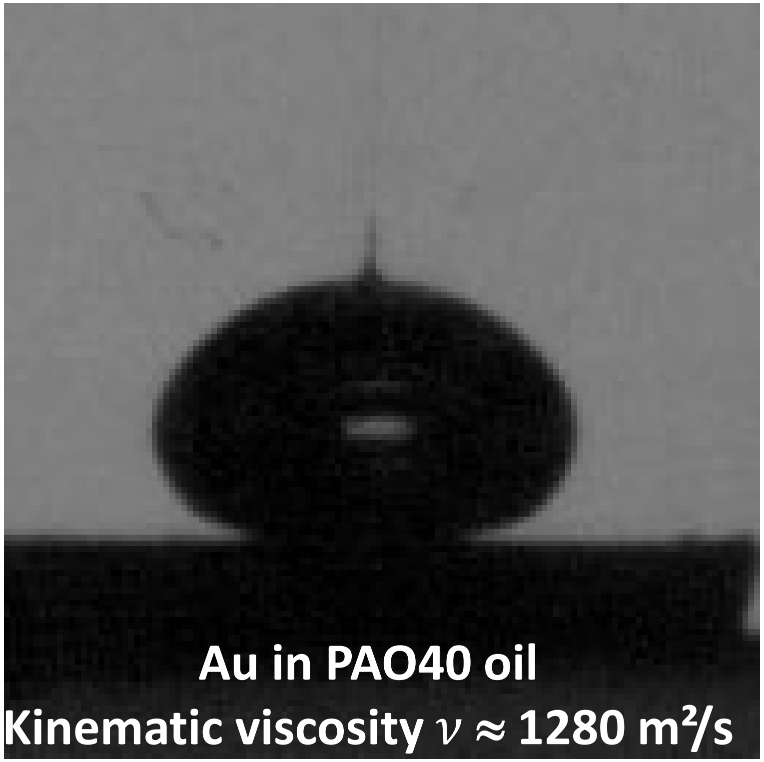

Huge capillary number $C_a = \frac{\rho \nu V_{cl}}{\sigma} > 100$, the contribution of the viscous forces to the friction drastically increases. The Rayleigh-Plesset and Gilmore are no more appropriate

T. Hupfeld et al., J. Appl. Phys. 127, 044306 (2020)

Direct resolution of the continuity and Navier-Stokes equations
(Finite volume method, *OpenFOAM* open source software @ https://www.openfoam.com/)

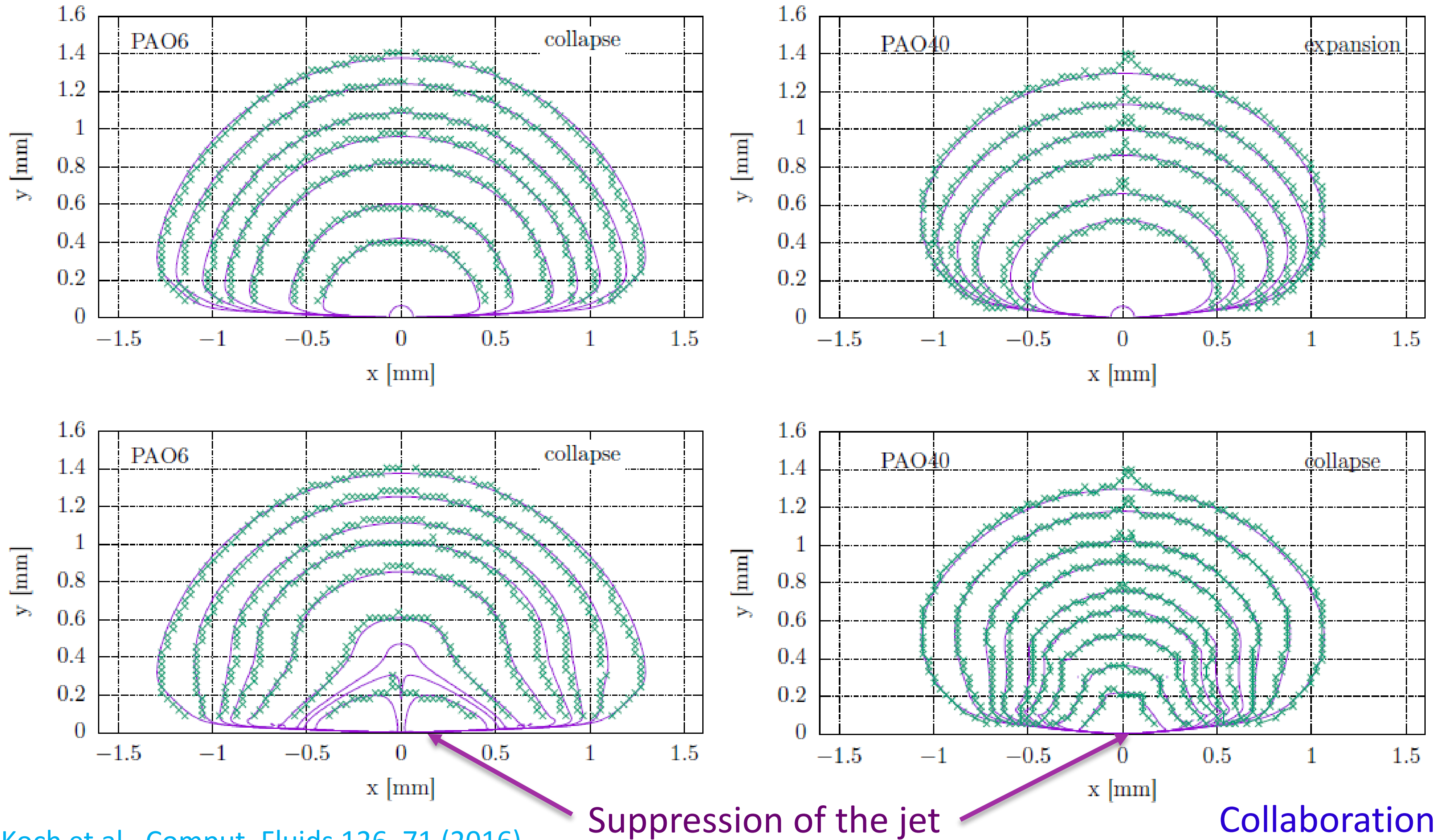

M. Koch et al., Comput. Fluids 126, 71 (2016)
C. Lechner et al., Phys. Rev. Fluids, 2020, 5, 093604.

Collaboration with
C. Lechner @ TU Wien

Conclusion

Thermodynamic parameters

Fast cooling 10 K/ns

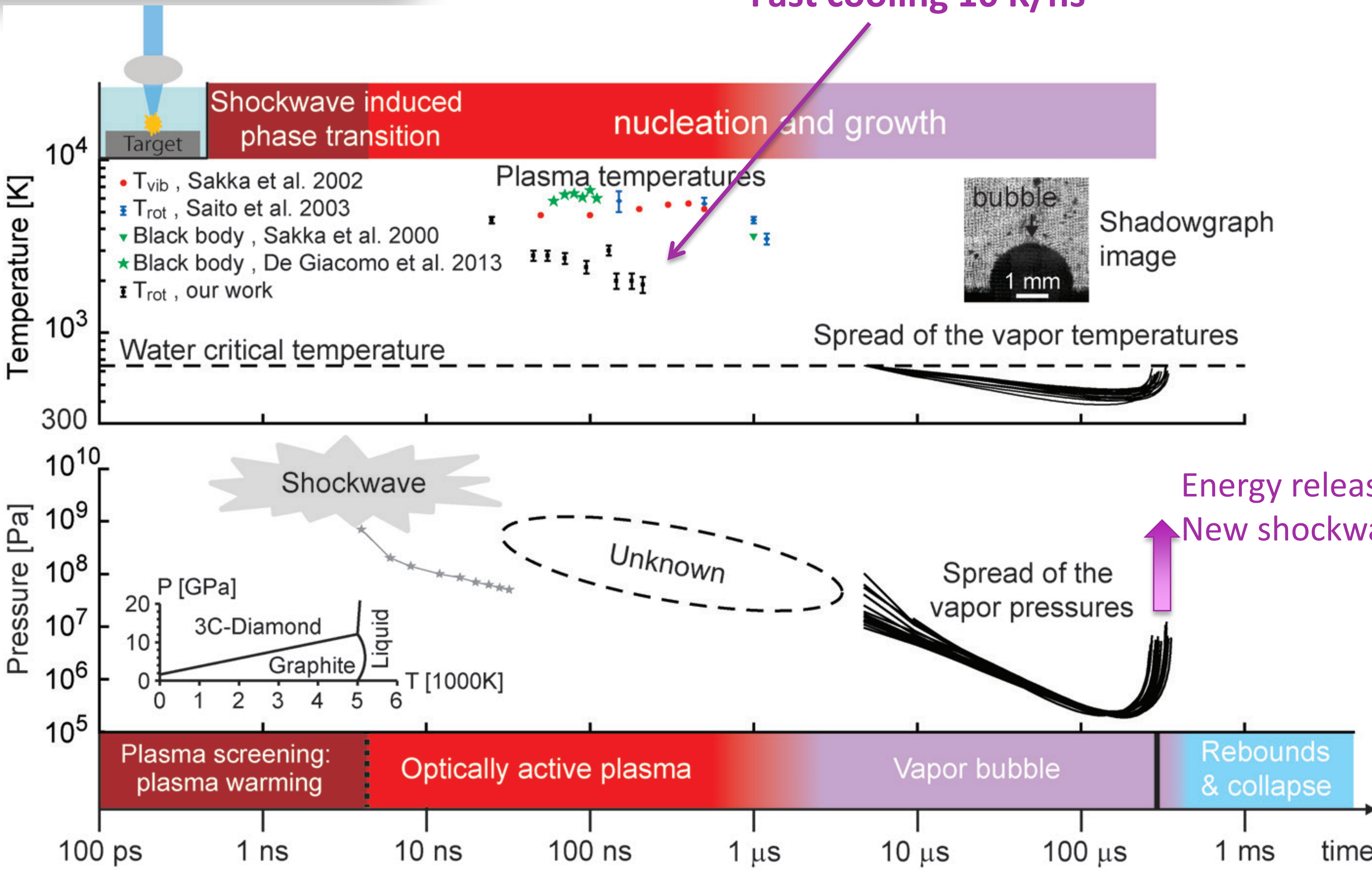

Energy release : New shockwave

D. Amans *et al.*, Origin of the nano-carbon allotropes in pulsed laser ablation in liquids synthesis, J. Colloid Inter. Sci. **489**, 114-125 (2017).

Acknowledgement

Institut Lumière Matière (ILM) , Univ. Lyon 1 / CNRS, France

Collaborators: Abdul-Rahman Allouche, Gilles Ledoux, Samy Mérabia, Vincent Motto-Ros, Christophe Dujardin, Amanda Ross, Sylvain Hermelin, Patrick Crozet.

PhD students: Julien Lam, Mouhamed Diouf, Gaetan Laurens, Arsène Chemin